INVESTIGATION ON MECHANICAL PROPERTIES OF 3D-PRINTED SINGLE STRUT

MUHAMMAD FAKHRUR IQBAL BIN MUSLIM

**A thesis submitted
in fulfillment of the requirements for the degree of
Bachelor of Mechanical Engineering (with Honours)**

Faculty of Mechanical Engineering

UNIVERSITI TEKNIKAL MALAYSIA MELAKA

2019

DECLARATION

I declare that this project report entitled "Investigation on mechanical properties of 3D-printed single strut" is the result of my own work except as cited in the references. The thesis has not been accepted for any degree and is not concurrently submitted in candidature of any other degree.

Signature :...

Name :...

Date :.......................................

APPROVAL

I hereby declare that I have read this project report and in my opinion this report is sufficient in terms of scope and quality for the award of the Bachelor of Mechanical Engineering (with Honours).

Signature	: ....
Name of Supervisor	: ……………………...
Date	: ....

DEDICATION

I dedicate this thesis to my beloved mother and father, Muslim bin Md Said and Jamiah binti Chek who have always been giving me spiritual support while they are living at hometown, Alor Gajah, Melaka. I am truly appreciate their loves and patients when educating me from time to time. I also dedicate this thesis to all my siblings (Razi, Ikram, Maizatul Anis) for being part of my life. My family has inspired me always and made me to be a better person in the future. Apart from that, I dedicate this thesis to my course mates and friends as they are willing to help whenever I have troubles in my life. They are rational to correct my mistakes and also give me some valuable advices.

ACKNOWLEDGEMENT

First and foremost, I would like to take this opportunity to express my deep appreciation to my supervisor Dr. Rafidah binti Hasan, from the Faculty of Mechanical Engineering Universiti Teknikal Malaysia Melaka (UTeM) for guiding me very well throughout this project. Under her supervision, I had gained her guidance and inspiration that enable me to complete this final year project successfully.

Moreover, I would like to express my greatest gratitude Dr Mohd Basri bin Ali as my panel seminar and also second report examiner. Next, I would like to express my deepest gratitude to Dr. Mohd Azli bin Salim as my second panel seminar. All of them are helpful and gave a great cooperation to ease my journey during accomplishing this study.

Furthermore, I would like to thank to Universiti Teknikal Malaysia Melaka (UTeM) especially the Faculty of Mechanical Engineering (FKM) for giving a fully support by allowing me to use their equipments and facilities during conducting my project.

In addition, I would like to express my sincere thanks to my friends and course mates for giving me their supports and advices in this project. Next, special thanks to my parents and my siblings for giving me their loves, supports and encouragements throughout this project.

ABSTRACT

This study focusses in producing tensile test specimen and method for the determination on the elastic property of 3D printed ABS single strut specimen. Designs of miniture single struts include a slender straight design with nominal strut diameter of 1.6 mm, total length of 24 mm, 45 mm, 50 mm, 75 mm and 90 mm. Compliance correction method is applied for single struts with different gauge lengths of between 8mm to 30 mm. Design of specimen is referred to ASTM E8/E8M-13a standard specification while tensile test is performed with reference to ASTM D638 standard procedure by using shimadzhu EZ test (EZ-LX) machine.

ABSTRAK

Kajian ini memberi tumpuan dalam menghasilkan spesimen ujian tarik dan kaedah untuk menentukan keupayaan elastik untuk spesimen strut tunggal daripada ABS yang dicetak melalui 3D. Reka bentuk miniture strut tunggal termasuk reka bentuk lurus langsing dengan diameter strut nominal 1.6 mm, panjang keseluruhan 24 mm, 45 mm, 50 mm, 75 mm dan 90 mm. Kaedah pembetulan pematuhan digunakan untuk struts tunggal dengan panjang tolok yang berbeza antara 8mm hingga 30 mm. Reka bentuk spesimen dirujuk kepada spesifikasi standard ASTM E8 / E8M-13a manakala ujian tegangan dilakukan dengan merujuk kepada prosedur standard ASTM D638 dengan menggunakan mesin shimadzhu EZ (EZ-LX).

TABLE OF CONTENT

LIST OF FIGURES

LIST OF FIGURES FOR APPENDICES

LIST OF TABLES

LIST OF ABBEREVATIONS

ABS	Acrylonitrile Butadiene Styrene
AM	Additive Manufacturing
BCC	Body Centered Cubic
CAD	Computer-Aided Design
CATIA	Computer Aided Three-dimensional Interactive Application
EBM	Electron Beam Melting
FDM	Fused Deposition Modelling
PLA	PolyLactic Acid
SEM	Scanning Electron Microscope
SLM	Selective Laser Melting
STL	Standard Tessellation Language

LIST OF SYMBOL

n	=	Nodes
p	=	Struts
m_b	=	Mass of block
ρ_s	=	Density of the steel
L	=	Length of cell
d	=	Strut diameter
x	=	Reading of measured diameter
N	=	Number of readings in a single strut
σ	=	Standard deviation
$\bar{x}$	=	Mean (average data)
%	=	Percentage difference
l	=	Evaluation length
E_u	=	Uncorrected modulus of elasticity
E	=	Modulus of elasticity
C_a	=	Apparent compliance factor
C_m	=	Machine compliance factor
δ_T	=	Total elongation

CHAPTER 1

INTRODUCTION

1.1 BACKGROUND

Lattice structure is a lightweight material. Many studies have done to determine mechanical properties of this material produced from stainless steel, aluminium, copper and other metals. Its properties of high stiffness and strength to weight ratio caused it widely to be used for lightweight structural applications (Doyoyo and Hu, 2006).

Lattice-structure comprises of many struts connected to each other by nodes, in many architectural arrangements such as body-centred-cubic (BCC), face-centred-cubic (FCC) and hexagonal close packed (HCP). These availabilities of joint type offer flexibility in assembly methods of the strut-based lattice structure. Hence, due to flexible configuration, the complex geometries design would prefer to apply the strut-based lattice structure (Doyoyo and Hu, 2006).

A node is a joint where two or more struts meet, and a strut is a link or member that connects two nodes. Many feasible options can be considered to define volume for designing strut-based lattice structures as it has variation number of nodes and struts to be combined. Figure 1.1.1 shown an example of lattice structure which consist of nodes (n) and struts (p).

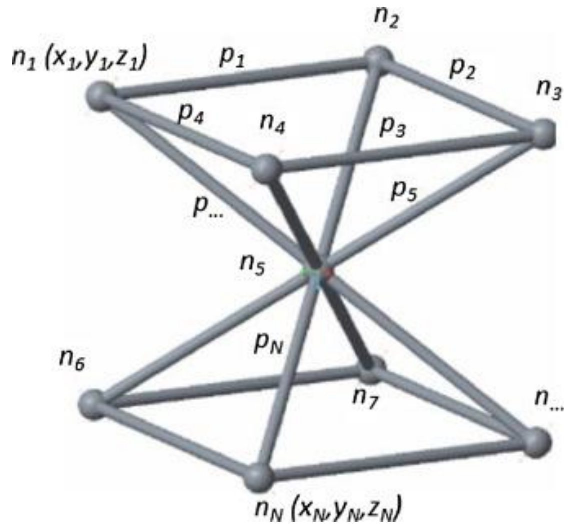

Figure 1.1.1: A strut-based lattice configuration with nodes n = 9 and struts p = 16.

(*Source: Syam et al., 2017)*

Certain process is needed in each fabrication method of lattice-structure material. There are various methods to produce lettice-structure material which are casting, wire bonding process, sheet metal forming and electron beam melting (EBM) (Rashed et al., 2016). One of the common method to produce lattice structure is casting method which is using injection moulding (Rashed et al., 2016). Wire bonding is generally considered the most cost-effective and flexible interconnect technology which is used to assemble the vast majority of semiconductor packages. Sheet metal methods is the process where producing lattice structure by press forming operation from a roll of sheet metal (Rashed et al., 2016). Otherwise in additive manufacturing (AM) techniques EBM is also one of the most selected method where the part is produced layer by layer (Rashed et al., 2016).

Additive layer manufacturing (ALM) or additive manufacturing (AM) is a modern fabrication process that can be use with wide range of materials to create product ranging from medical implants to parts of an aircraft wing. 3D printing is one of the categories in additive layer manufacturing available which the printed part is formed layer by layer (Gebhardt, 2003). The first step in fabricating parts by using this technology is to create the required geometry layer by layer, using computer aided design (CAD) data. Due to the high process flexibility and the possibility to produce parts with a high geometric complexity, AM technology is an advanced method that used widely

1.2 PROBLEM STATEMENT

Mechanical properties especially modulus of elasticity, yield strength and maximum strength of lattice structure materials can be obtained through stress-strain diagram. In case for lattice-structure materials arrangement, compression test is one of the simplest methods to obtain the stress-stress diagram. However, using compression test will not give the failure strength and failure strain data. Tensile test is preferred to provide the failure data. For micro-lattice structure as a whole, tensile test experiment will need a specially designed and fabricated jig to hold the specimen. To simplify this, it is suggested that tensile test on single strut specimen need to be done.

Stress-stress diagram for single strut can provide some information related to the basic failure of lattice structure material. For ABS lattice-structure fabricated using 3D printer, mechanical properties from tensile test has not yet been conducted. Thus, this study is looking for such data.

1.3 OBJECTIVE

To investigate mechanical properties of 3D printed single strut with selected parameter using tensile test.

1.4 SCOPE OF PROJECT

The scopes of this project are:

1. Design of single strut for tensile test specimen using Solidworks with selected parameter.
2. Fabrication of single strut tensile test specimen using CubePro 3D printer, from ABS material.
3. Conduct tensile test experiment for single strut by using Shimadzu table top machine.
4. Analyse mechanical properties of single strut using compliance correction method.

CHAPTER 2

LITERATURE REVIEW

2.1 Introduction

In this chapter, the background of this study will be researched in order to have better understanding of fundamental knowledge before proceed for further progress. All topics are which relevant with this study are discussed based on the journal articles and academic book. Besides that, all materials from previous research which related to this study will be described as well.

2.2 Lattice-structure and Strut

Struts is the basic units which will be connected to each other to form lattice structure. The connection between struts are called nodes, the point where struts meet together in the structure. In a fixed volume, there are various types of configuration where strut-based lattice structure can be designed with variation of node position. Material used in the lattice-structure can be saved as it has high stiffness to weight ratio. Hence, the problem of forming in any complex geometries can be eliminated when the strut-based lattice structure is applied (Doyoyo and Hu, 2006).

Large number of formations of strut-based lattice structure in a fixed volume can be deformed when the number of nodes and struts are not fixed. Node position and strut diameter also can be the variable in a specific volume besides the alteration of number of nodes which can produce large number of results (Syam et al., 2017). Strut-based lattice structure can be in numerous form such as cubic truss and octetruss as shown in Figure 2.2.1.

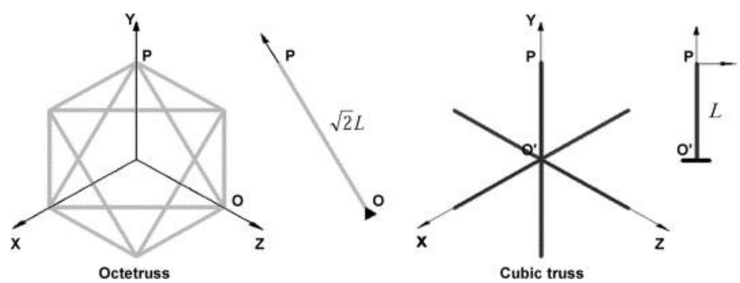

Figure 2.2.1: Octetruss and cubic truss.

(Source: Doyoyo and Hu, 2006)

2.3 Methods in Producing Lattice-structures

Common process to manufacture lattice-structures are through casting, sheet metal forming or wire bonding process. These regular assemblies are time-consuming and furthermore limited the complexity of lattice-structure designs. These methods are just used to produce lattice-structure materials with simple setup on a macroscale (Tang et al.2017).

In casting process, ceramic casting slurry is used to coat a pattern of wax or polymer lattice-structure. This ceramic is a mold and the wax or polymer is the expelled through the process of melting. The liquid metal with high fluidity can be utilized to fill in the vacant shape of the mold to form lattice-structure material. Wide range of shapes of lattice structure can be formed by using this method as any shape can be produced according to the designed mold. Through out this process, the produced lattice-structure material had severe porosity and this method is time consuming and costly. Example of octet-truss lattice structure produced from casting process is shown in Figure 2.3.1.

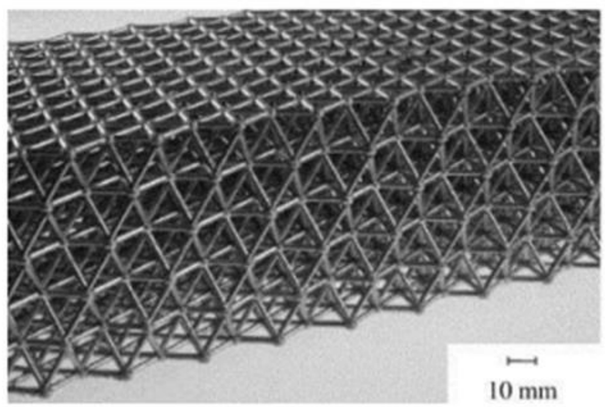

Figure 2.3.1: Octet-truss lattice structure.

(Source: Rashed et al., 2016)

For sheet metal forming procedure, a roll of sheet metal is experienced perforation punch to form the shaped holes such as diamond or hexagonal. The annealing process is used to treat the elongated perforated sheet which can soften the struts before proceed to punching process. The sheet then being bent with the combination of die and punch. Step in punching process enables the perforated sheet to be grooved. Subsequently, a simple lattice-structure material can be fabricated through these procedures from a sheet metal. Figure 2.3.2 demonstrates the procedures of sheet metal forming method (Rashed et as.,2016).

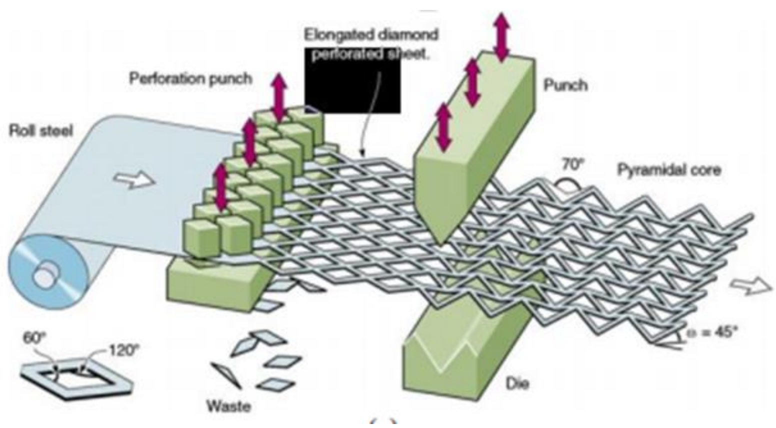

Figure 2.3.2: Sheet metal forming process.

(Source: Rashed et al., 2016)

In any case, the presentation of additive manufacturing (AM) technologies had reduced the restrictions in creating lattice-structure materials. AM technologies fabricate a section layer by layer empowers the design of lattice-structure materials in complex arrangement. Through this technology, any complex of lattice-structure can be produced easily and also in variation of geometrical scales such as microscale, mesoscale or macroscale (Reinhart et al., 2012).

2.4 Additive Layer Manufacturing

Commonly, the first step in AM technology is designing the 3D model using a CAD (Computer-Aided Design) software. The completed 3D model then will be saved into a "STL" (Standard Tessellation Language) file format which is developed from 3D Systems. This STL file will be read by computer for data preparation to create slices of the model. The data will be sent to a program of an AM machine for creating the structured part. For removing the model from its support structure, a post process is needed to maintain the specification of the designed model (Kessler et al.,2016).

One of the famous additive layer manufacturing technologies is 3D printing. There are various types of 3D printing which classified by the use of raw materials such as solid-based, powder based or liquid based (Gebhardt, 2003). A single strut which is the basic element of lattice structure can be created by utilizing 3D printing that offered fabricating layer-by-layer (Kessler et al.,2016).

There was a research on fabricating strut shape of lattice-structure using SLM (selective Laser Melting) method which is powder-based AM technology (Kessler et al., 2016). The raw material used in this method is metal powder. In this SLM process, a thin powder layer was stored, and CO2 (carbon dioxide) laser was lighted to the powder surface progressively until the final part was produced based on CAD data. It concentrated on few types of cross sectional state of swaggers and its achieved quality. The analyzed shapes were elliptical, square, circular, rhombus and triangular. The limitation of SLM process were evaluated during the producing of these struts. One of the limitation for circular cross section that can be discussed was the nominal diameter which cannot be build smaller than 0.15 mm (Kessler et al., 2016). The fabricated struts with different diameters was shown in figure 2.4.1.

Figure 2.4.1: Fabricated struts with different diameters.

(Source: Kessler et al., 2016*)*

In utilizing the SLM process, there was included the study of stainless-steel micro-lattice block structure. The diameter in a Body Centered Cubic (BCC) micro-lattice structures which made by stainless steel in SLM process can be calculated by a derived equation. This equation literally used for fabricated micro-lattice block structure with different SLM process parameter to observe its strut diameter as shown in equation 3.1 (Tsopanos et al., 2016). According to the equation expressed, m_b is the mass of block, ρ_s is the density of the used steel, the N_1, N_2, N_3 are the quantity of cells along the width, length and height directions, L is the length of cell.

$$d = \sqrt{\frac{m_b}{\rho_s . \pi . N_1 \times N_2 \times N_3 . L . \sqrt{3}}} \qquad [3.1]$$

2.5 Polymer 3D Printer

In this analysis, struts arrangement are manufactured by polymer 3D Printer and utilizes FDM (Fused Deposition Modeling) procedure. Firstly, the plastic material in form of filament is melted then will be extruded as semi-liquid materials. The expelled material will be cool down by the environment and solidified to form the designed model. The process took place layer-by-layer to ensure the exactly desired geometrically. Material strength, layer thickness, envelope temperature and deposition speed are some parameters that need to be concerned to allow the performance functionalities of the system operate optimally.

CubePro Printer has been chosen among other 3D printer for being use in this study. This is because of its suitable features for this study which equipped with ultra-high-resolution setting of 300 microns, 200 microns and 70 microns print layer thickness. Furthermore, it is also has good accuracy for print the model in detail form with helped from the build in Z axis resolution of 0.1mm feature. The maximum operating temperature will be 280^{o}C at the extruder tip and 15mm per second is the maximum deposition speed. PLA (polylactic acid) or ABS (acrylonitrile butadiene styrene) were the raw material used for this CubePro Printer (3dsystem, 2018). The actual CubePro Printer is shown in figure 2.5.1.

Figure 2.5.1: CubePro 3D printer.

2.6 Fundamental of Tensile Test

Tensile test was set to use in this research to investigate the mechanical properties of single struts. Information on the strength and ductility of materials under uniaxial tensile stress can be obtained from this test. It is a simple testing that can be performed quickly to gain the result. First of all, the tensile test machine needs to be set with the constant load and the gauge length accordingly to the prepared data. Then, the fabricated single strut was securely held by top and bottom grips attached to the tensile testing machine. Once the tensile test started, the grips were moved apart at a constant rate of load which pull the specimen apart as well. A computer which connected to the tensile test machine will continuously recorded and plotted on a stress-strain curve until failure based on its displacement and force applied (Halil et al,. 2013).

A small bench top servo-hydraulic testing machine (Shimadzhu EZ-LX) was selected to be used in this study. One of the reasons to choose this type of tensile test machine is because the test can be run at high-precision load cell that make sure accuracy to within 0.5% of indicated value over a wide range from 1/500 to 1/1 of the load cell capacity. This feature help to obtain the accurate value during the test.

Among their model, EZ-LX has the higher tester load capacity which is up to maximum 5 kN and it is suitable to test the single strut properties (Van et al,. 2015). The crosshead speed range offered by this model is within 0.001 to 1000 mm/min. Total time taken to run the whole test also can be reduced because of its high return speed which 1500 mm/min. On the other hand, this Shimadzu model was a very user-friendly machine as the user can run the test by following the user manual besides equipped with automatic calibration by using calibration cable. Trapezium X is the software that work together with this machine to interpret the data from the tensile test (Shimadzhu, 2018). Figure 2.6.1 shows the Shimadzu EZ-LX model that used to run tensile test for the single struts.

Figure 2.6.1 : Shimadzhu EZ-LX tensile test machine

(source : Shimadzhu 2018*)*

2.7 Conclusion of Chapter 2

In summary, the relevant journal, book and articles help in reviewing the background of this study. The related knowledge gained are applied through this study such as limitation of AM process in producing struts and all the equation used for characterize the struts. The methodology of this study is planned after the background of this scope is understood completely.

CHAPTER 3

METHODOLOGY

3.1 Introduction

In this chapter, a workflow is decided and presented for conducting the study. A series of processes need to be carried out which first of all is to design single struts. After that the designed structure need to be fabricated according to their geometry. The last process is to test the single strut under tensile test and analyze the result. Every detail of each process is explained in this chapter.

3.2 Workflow Chart

Every step and process which need to be done for accomplishing this study are listed as below. Figure 3.2.1 presents the flow chart of methodology in this study. Initially, all journals, articles and materials which relevant to the study are gathered and literature studies are conducted to review 3d printing and single strut. After that, by using computer-aided design (CAD) which is CATIA, the single strut is designed with 1.6 mm diameter and 35.26^{o} build angle. The designed single strut then be fabricated by using 3D printer which is the CubePro machine. Next, all the single strut which perfectly fabricated as in the drawing are tested for tensile test with different gauge length. All the data from the test is evaluated by using compliance correction method and observed for the test failure by using portable optical microscope which is Dino-Lite Pro. At the end of this study a report will be written. At the end of FYP 1 the preliminary results are obtained at the fabrication stage. In this FYP II, all single struts should be confirmed to be printed successfully based on their designs before proceed to testing stage.

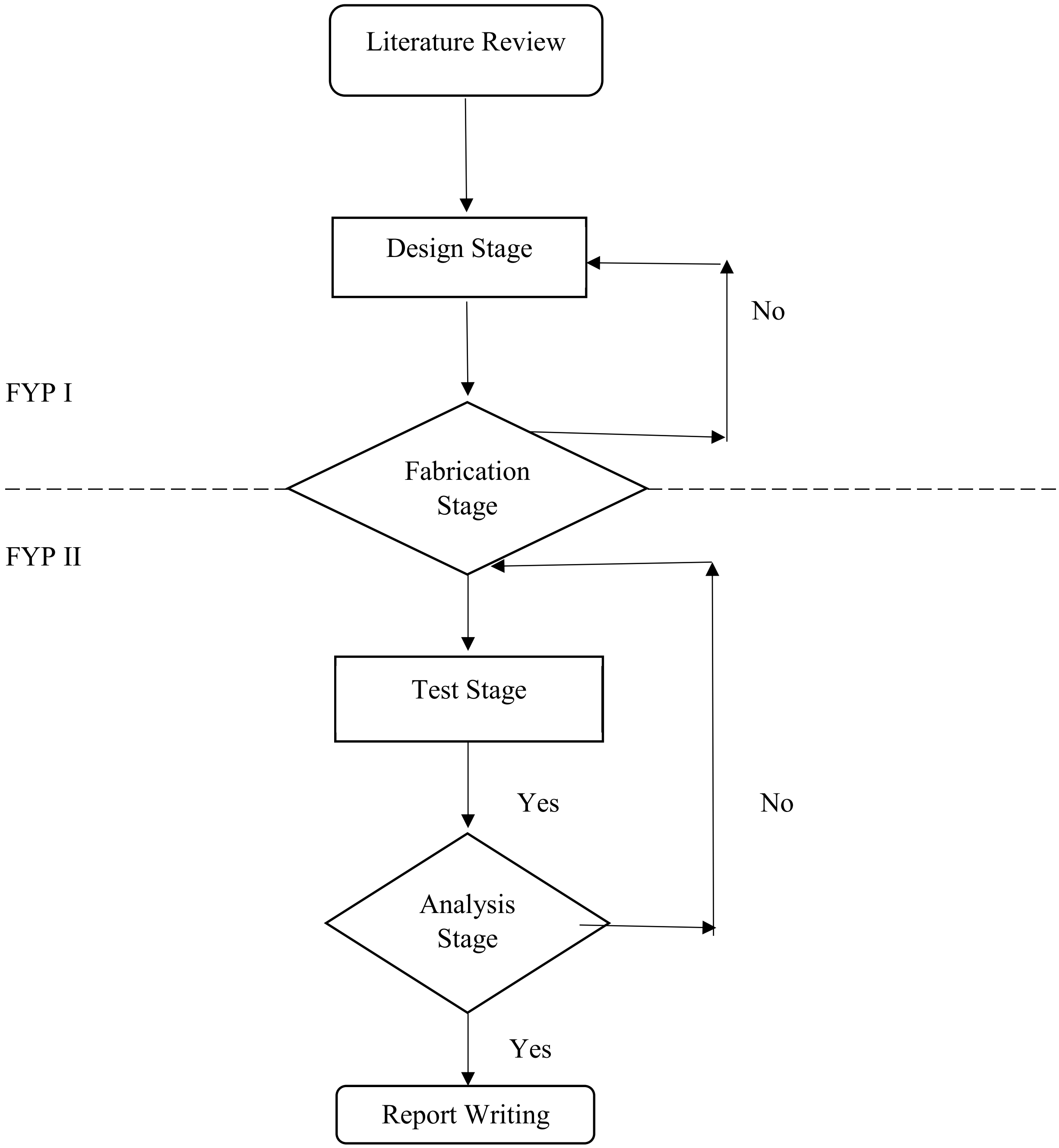

Figure 3.2.1: Flow chart of methodology

3.3 Design Stage

Table 3.3.1 shows all the specimens according to their parameter which is gauge length.

Table 3.3.1: Parameters of single struts

Diameter (mm)	1.6				
Built angle from horizontal (◦)	35.26				
Specimen length (mm)	24	45	50	75	90
Gauge length (mm)	8	15	20	25	30
Number of specimens	3	3	3	3	3
Total number of specimens	15				

The parameters of the single struts are set to have five different gauge lengths which are 8 mm, 15 mm, 20 mm, 25 mm and 30 mm. The gauge length is designed to be one-third of total specimen length. This is due to common ratio of standard tensile test specimen. Therefore, the specimen length also varied for all gauge lengths, and becoming one of the parameters to ensure the specimen is able to be hold perfectly in the tensile test. The diameter of the struts is fixed with 1.6 mm each as it is a reasonable value to obtain good mechanical properties result. In fact, the built angle from vertical is chosen as 35.26° as it represents the angle of the struts to the surface in BCC structure. Three specimens for each parameter are produced and undergoes tensile test, so there are 15 specimens in total to be fabricated.

All the single struts are designed and drawn using a CAD software which is CATIA. Figure 3.3.1 shown an example of a part drawing and Figure 3.3.2 until Figure 3.3.6 shown each dimension of the single struts. Each single strut drawn with a side support to ensure the strut can be printed successfully. After the struts are completely designed in 3d modelling, the drawing is then converted in to “STL” (Standard Tessellation Language) file format in Catia software. After that, the STL file is then transferred to the software of CubePro to create slices from the model of single struts for data preparation before producing the single struts.

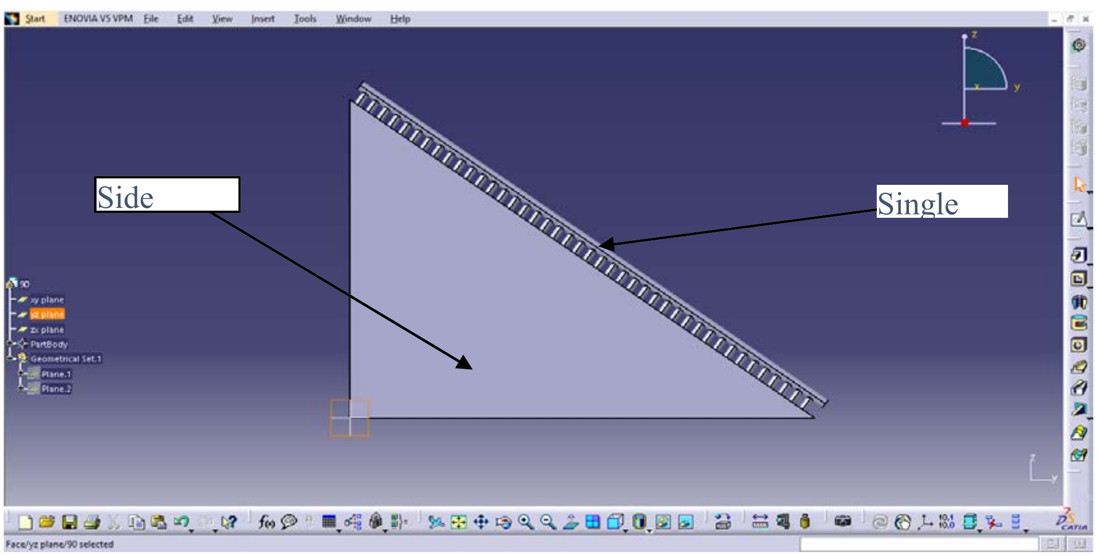

Figure 3.3.1: The part drawing of single struts in Catia

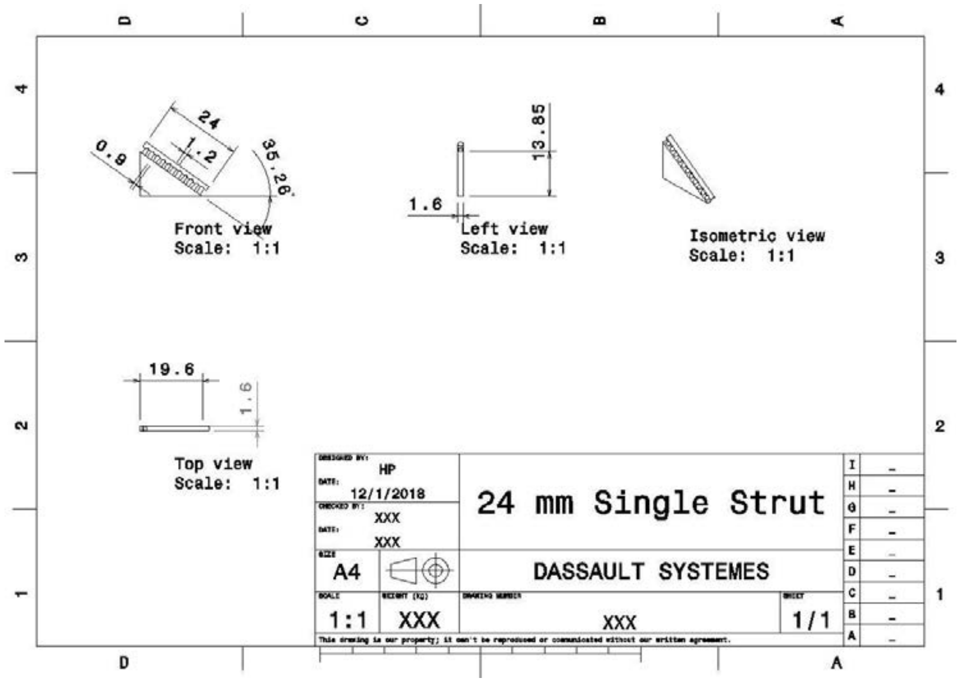

Figure 3.3.2: The dimension drawing of 24 mm single strut in Catia.

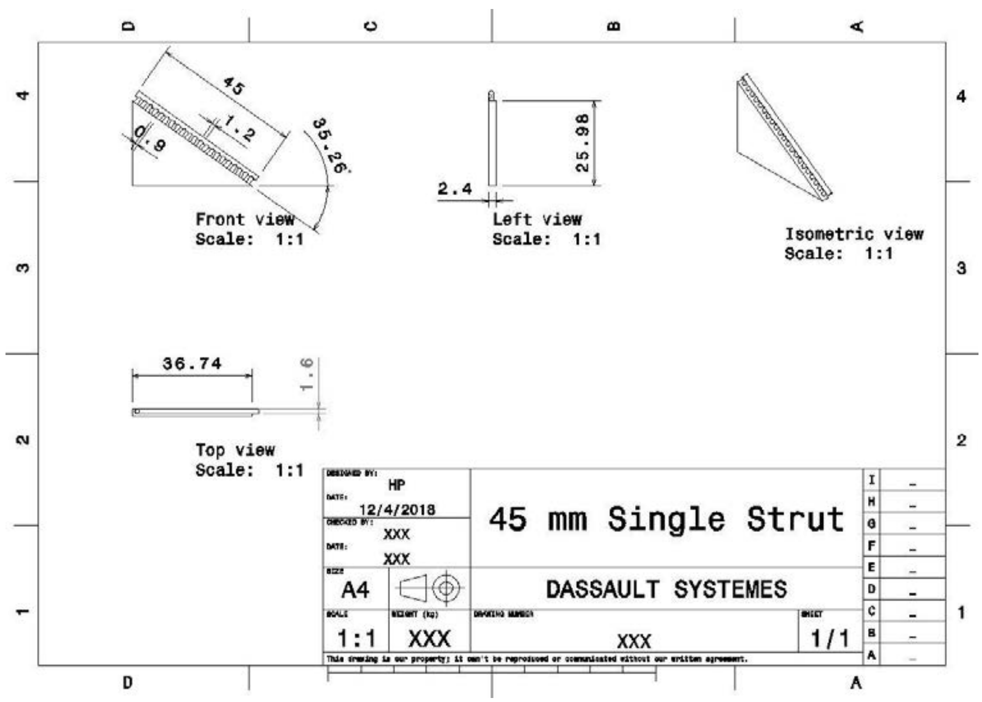

Figure 3.3.3: The dimension drawing of 45 mm single strut in Catia.

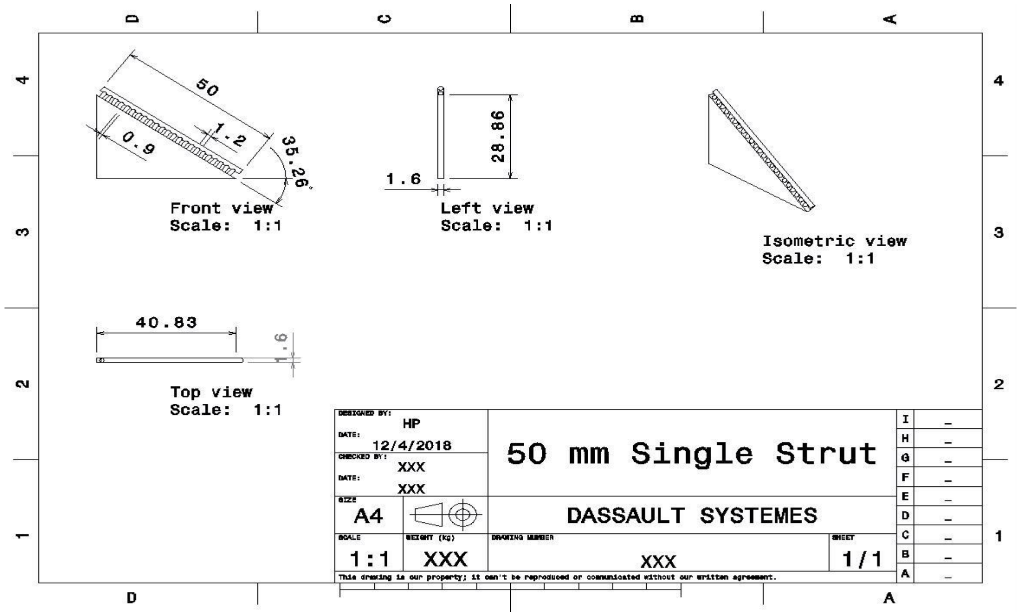

Figure 3.3.4: The dimension drawing of 50 mm single strut in Catia.

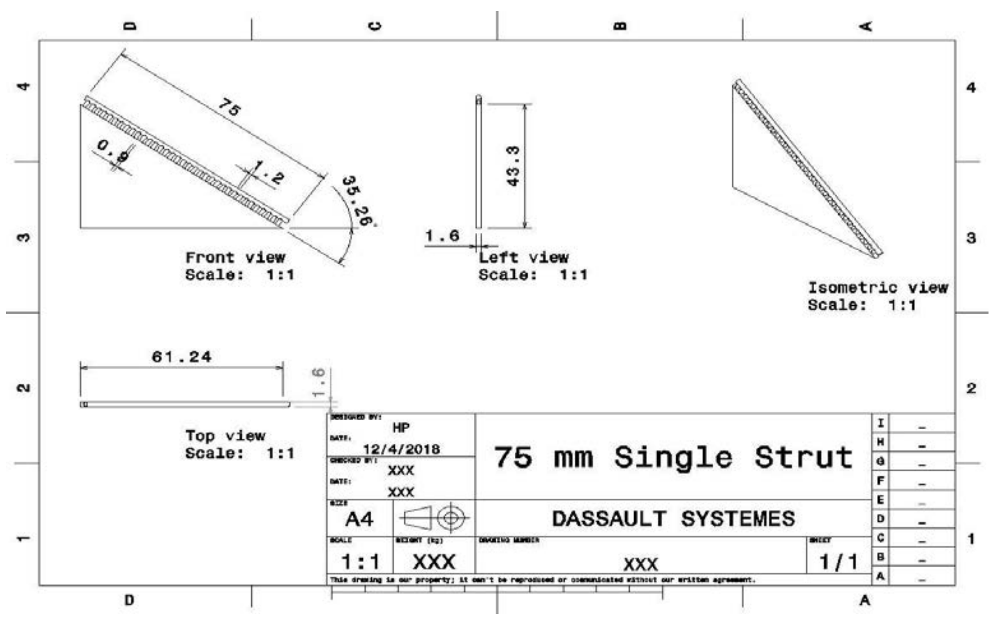

Figure 3.3.5: The dimension drawing of 75 mm single strut in Catia.

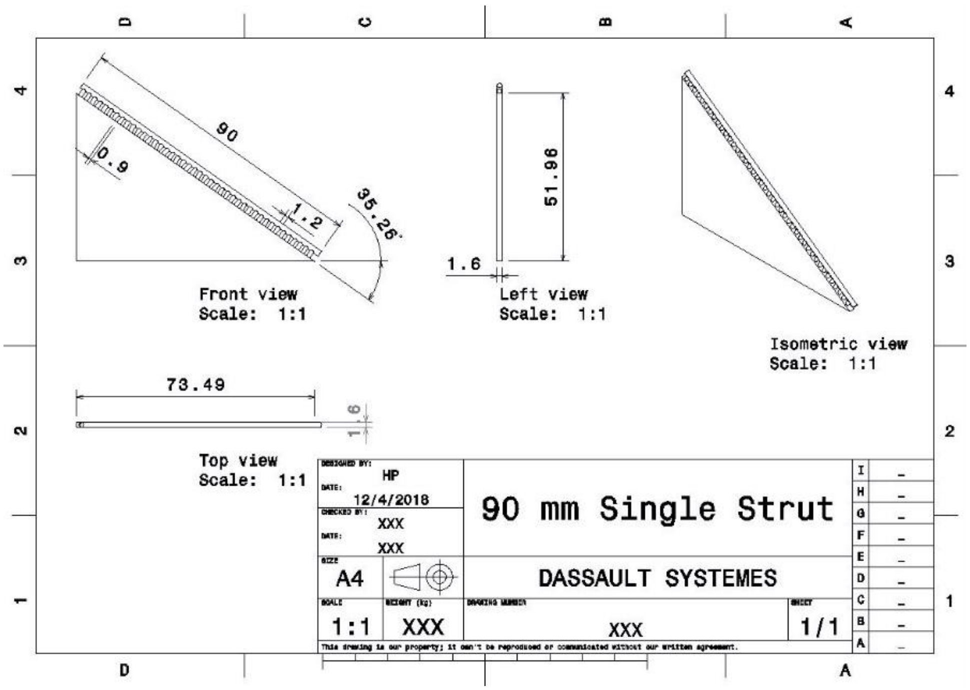

Figure 3.3.6: The dimension drawing of 90 mm single strut in Catia.

3.4 Fabrication Stage

There is a build setting to create slices of the model of single struts once the selected STL file is opened in the CubePro software for being built layer by layer during later 3D printing process. Several process parameters can be chosen for printing the designed model from the build settings. Figure 3.4.1 and 3.4.2 show the build settings and their descriptions of CubePro software which the bottom supports of single struts are generated automatically during the fabrication. Figure 3.4.3 show the CubePro software create slicing virtually.

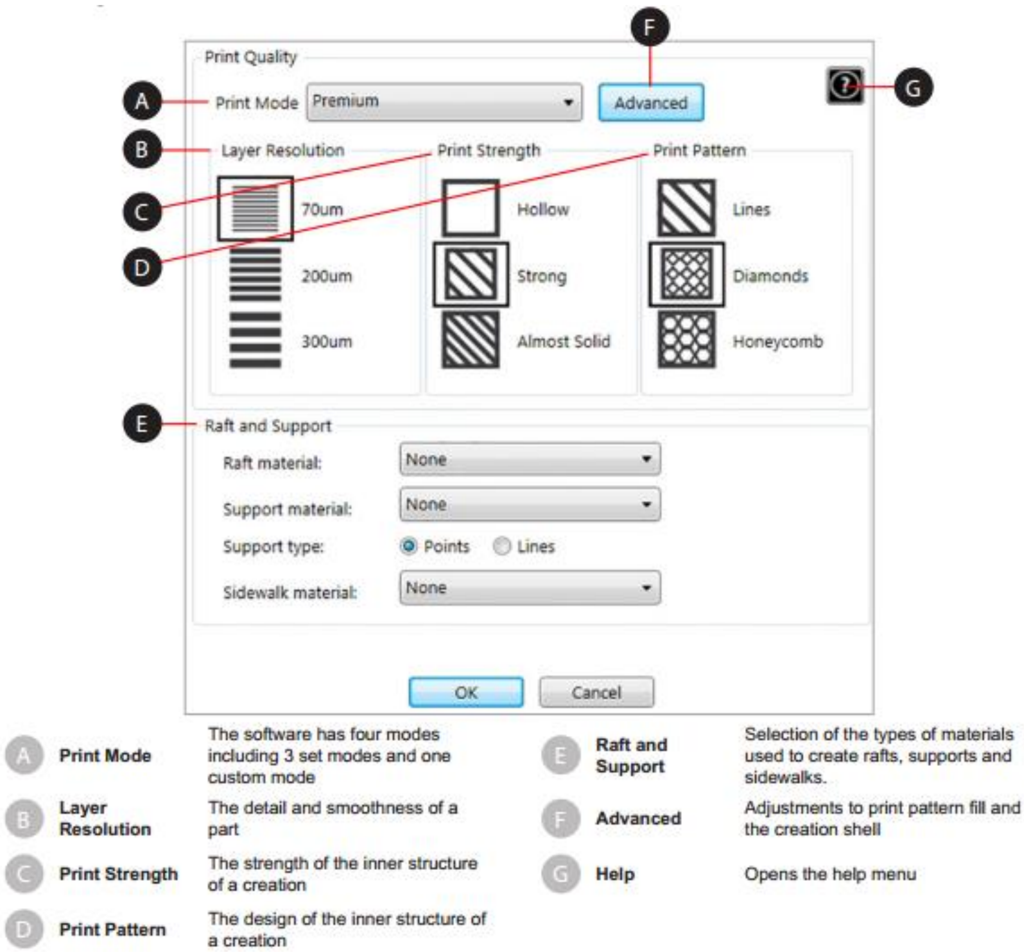

Figure 3.4.1: Build settings of CubePro software.

(Source: 3D Systems Inc., 2015)

Print Mode		
	Standard	• Layer Resolution: 200um • Print Strength: Strong • Print Pattern: Diamonds
	Premium	• Layer Resolution: 70um • Print Strength: Strong • Print Pattern: Diamonds
	Draft	• Layer Resolution: 300um • Print Strength: Strong • Print Pattern: Lines
	Custom	Custom allows the user to customize their print settings
Print Resolution		
	0.070	• Great mode for parts requiring smooth surfaces • Layer lines are not very visible in these parts • Good mode for artistic parts with a smooth flow • Not the best mode for fine detail
	0.200	• Best mode for general printing and most compatible mode for a wide range of geometries • Fine detail preservation for things like steeples, spires, sharp points, or thin walls
	0.300	• A fast mode with thicker layers • Good for large parts with minimal detail
Print Strength		
	Hollow	• Fastest mode to produce a part • Hollow has fewer outer surfaces and larger print pattern spacing • Best for parts that will not be stressed
	Strong	• Medium amount of outer surfaces and smaller print pattern spacing • Best for parts that will have minimal physical abuse
	Almost Solid	• The most surfaces and the tightest print pattern spacing • The most robust part • Best for parts that will be stressed
Print Pattern		
	Lines	• Fastest print fill pattern • Minimal cross bracing
	Diamonds	• Strong print pattern with 2-direction cross bracing
	Honeycomb	• Strong print pattern with 3-direction cross bracing

Figure 3.4.2: Descriptions on the build settings.

(Source: 3D Systems Inc., 2015)

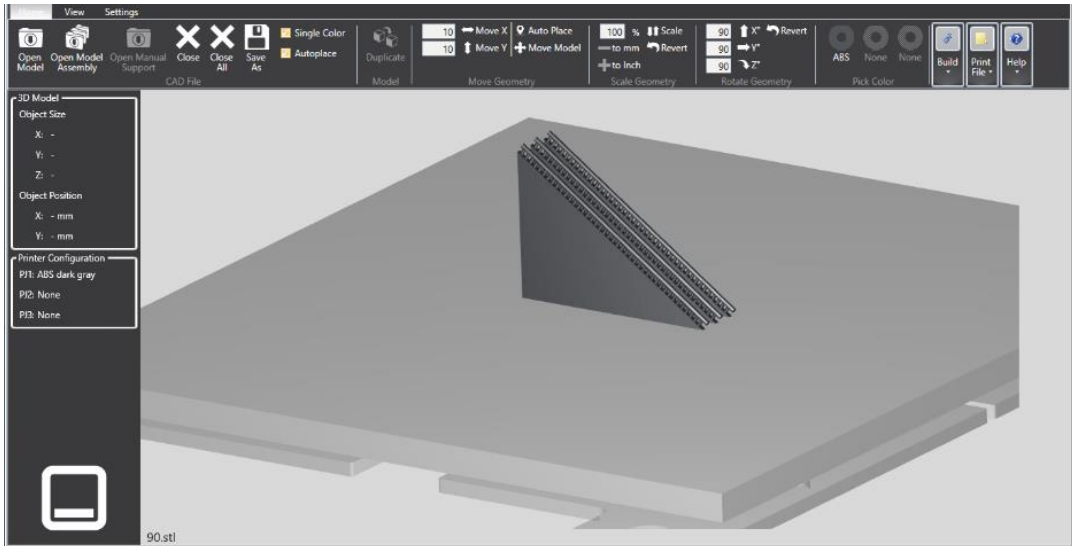

Figure 3.4.3: Single struts in CubePro software to create slicing.

Table 3.4.1: Process parameters selected for single struts

Strut length (mm)	Layer Resolution (µm)	Print Strength	Print Pattern
24	200	solid	Cross
45	200	solid	Cross
50	200	solid	Cross
75	200	solid	Cross
90	200	solid	Cross

The process parameters are selected as shown in Table 3.4.1 for the formation of the single struts in this study. Based on the description in Figure 3.4.2, the suitable for wide range of parameter is 200 µm layer resolution despite the solid is the strongest form to be printed. Moreover, a preliminary run has been carried out and 200 µm resolution with cross print pattern was give desired result, this is similar to the work that has been done by Yin Cheng (2018). After the selections of the build settings is completed, the platform of the printing bed must be ready by applying the Cube Glue. This procedure is to make sure the printed part is fix without moving from the platform during the printing process.

The printing bed and the nozzle then being heat up to the predetermined temperature. Next, the printing process is ready to start. The materials are extruded in molten form through this process, therefore the temperature of the nozzle is just below the melting point of the ABS material used in this process. Figure 3.4.4 shows three sets of identical single struts which were being fabricated at once according to their parameters in each process which can reduce the time taken for printing.

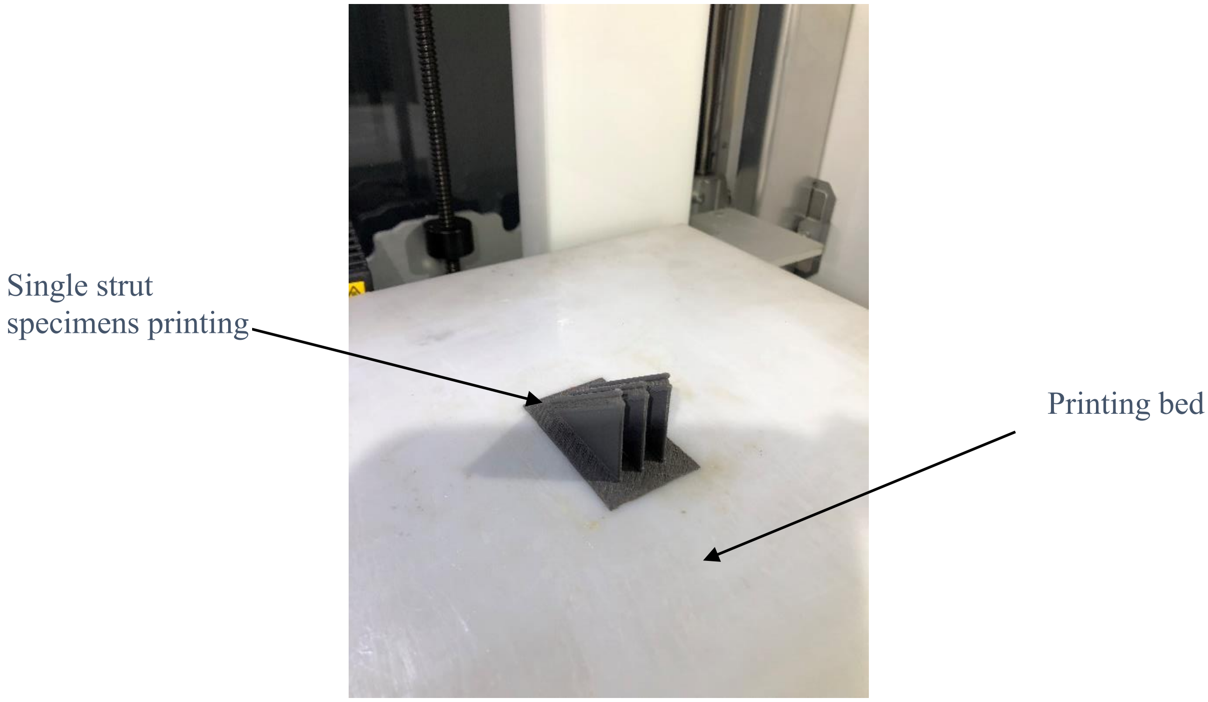

Figure 3.4.4: Fabricated single struts in CubePro 3D printer.

After the 3D printing process is completed, the single strut needs to be separated from its built supports in preparation for tensile test. As the bottom support is very thin and flimsy which auto-generated by Cube Pro software, it can be easily detached by hand ss shown in Figure 3.4.5. For the side support, trimming knife is used to cut off all of it as in Figure 3.4.6. The single struts then need to be trimmed all the tiny supports left on its surface by using trimming cutter which clearly shown in Figure 3.4.7. This trimming process must be done carefully to ensure the single strut is not damaged. Next, all the single struts are labelled by its length using masking tape and ball pen as shown in Figure 3.4.8 (a) and (b) for easy recognition. Figure 3.4.9 shows the completed five sets of printed single struts.

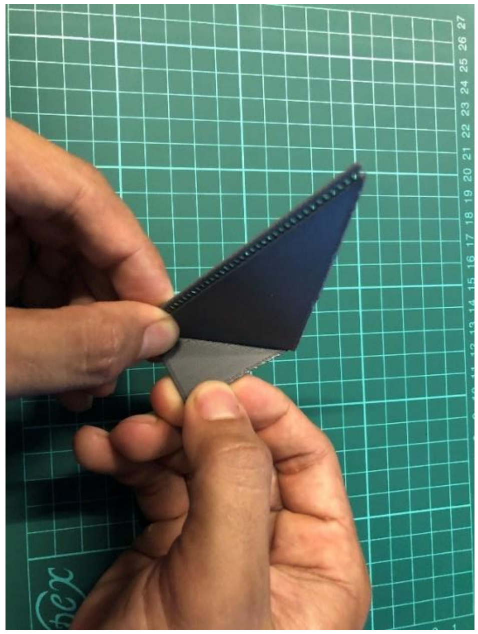

Figure 3.4.5: Detach the bottom support.

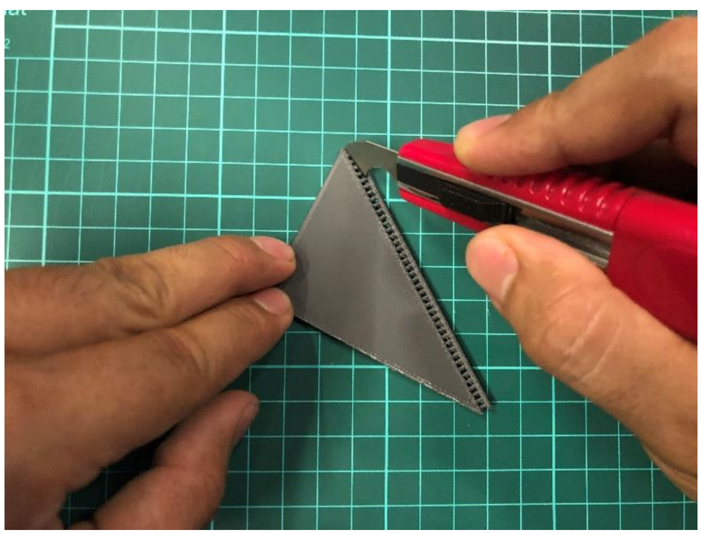

Figure 3.4.6: Cut off the side bottom.

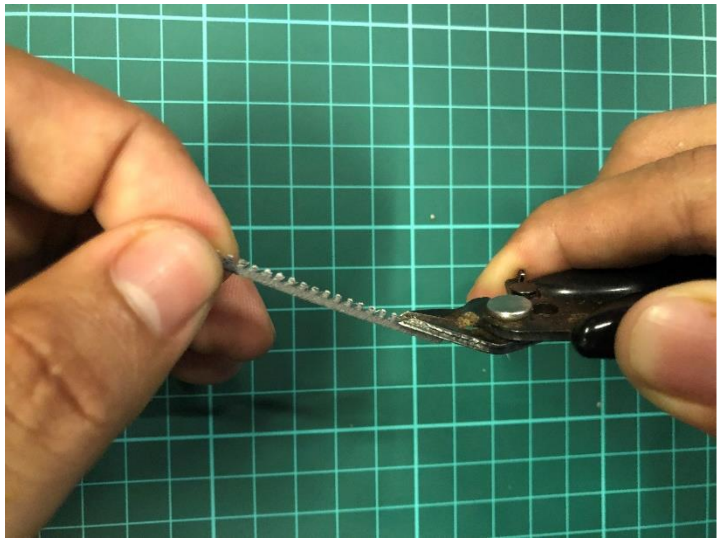

Figure 3.4.7: Tiny supports are cut.

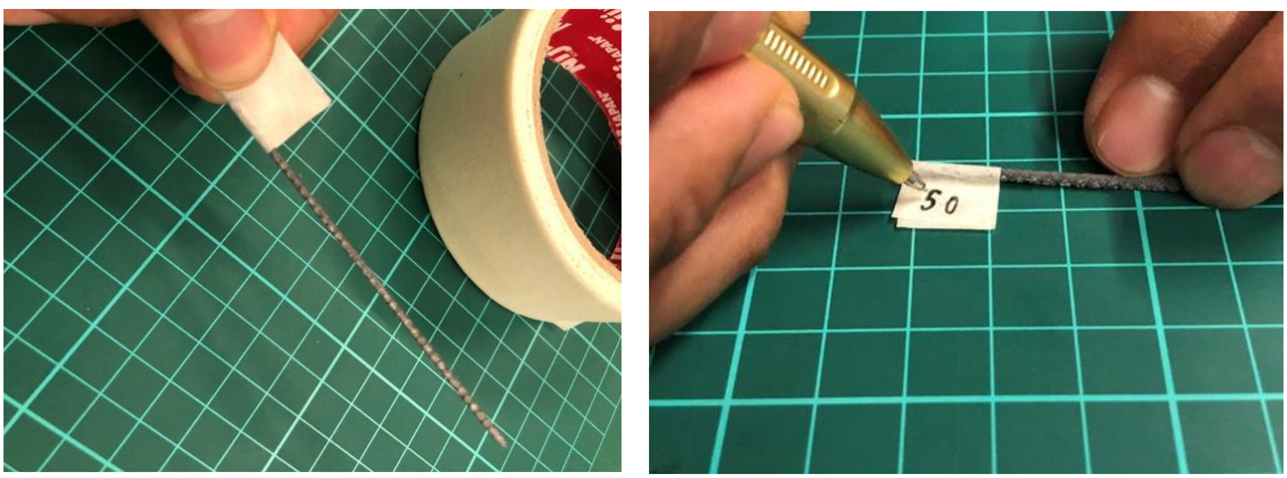

a) b)

Figure 3.4.8: Single strut is labelled using (a) masking tape and (b) a ball pen.

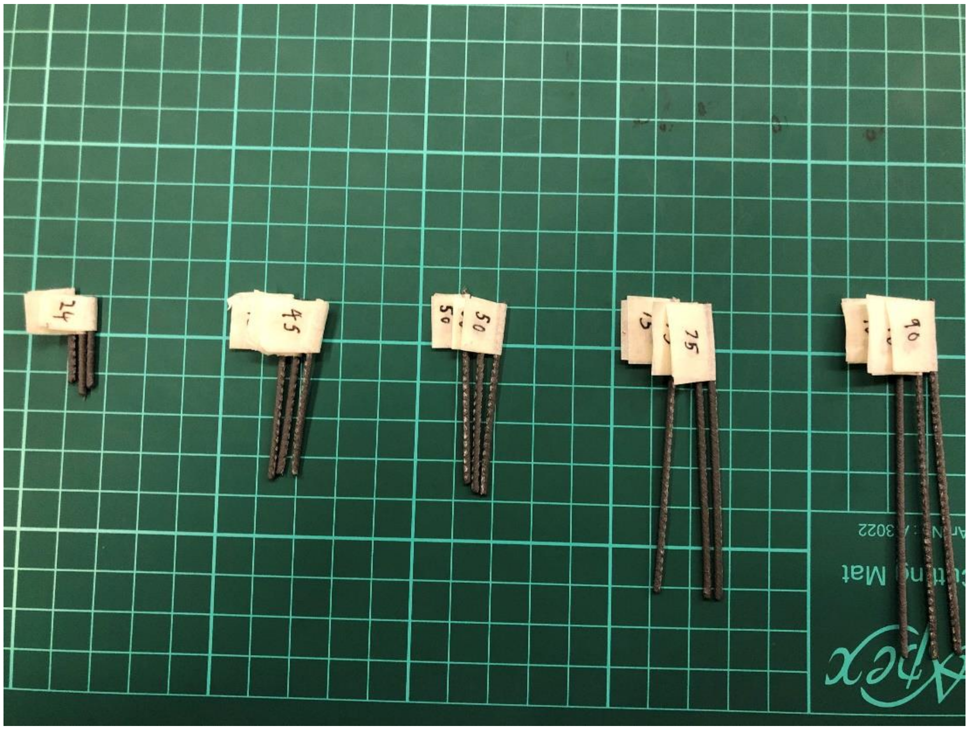

Figure 3.4.9: Five sets of printed single struts.

3.5 Test Stage

After all single struts are completely ready with the desired shape and parameter, Dino-lite pro will be used in characterization test to observe the appearance of fabricated struts. This microscopic equipment has variable magnification from 10 times up to 220 times as well with provided software for computer in order to capture image and for measuring purposes. A single strut is placed under the microscope as shown in Figure 3.5.1.

Figure 3.5.1: Single Strut is placed under Dino-Lite Microscope at 45 times magnification to determine its charachteristic.

The tensile tests for the single struts were conducted on a small bench top servo-hydraulic testing machine (Shimadzu machine controlled by a computer using Trapezium software) with 1 kN load cell, due to the small size of the single struts. Loading velocity of 0.1 mm/minute was applied throughout the test, without the application of extensometer for strain measurement. The load was recorded by a dedicated computer in a graph and table form. The strain was derived directly from the crosshead displacement whereas, the stress can be determined by dividing the force over cross-sectional area of the single strut. Then, the compliance correction method was applied from the calculated data.

In this study, five different gauge lengths were tested; 8 mm, 15 mm, 20 mm, 25 mm and 30 mm, with three repeat tests for each gauge length. Figure 3.5.2 shows the arrangement of the machine for the tensile tests by using Shimadzhu machine. The gauge length measurements were set by using a ruler and for repetition tests, the setting measurements at the machine were used. This mean that for each gauge length, a same measurement length was used in all repetitions. Both specimens end were manually tightened at jaw grippers. From the preliminary test that have been done before, the result show that there were no slippery problem with the jaw grippers and the test can be done effieciently.

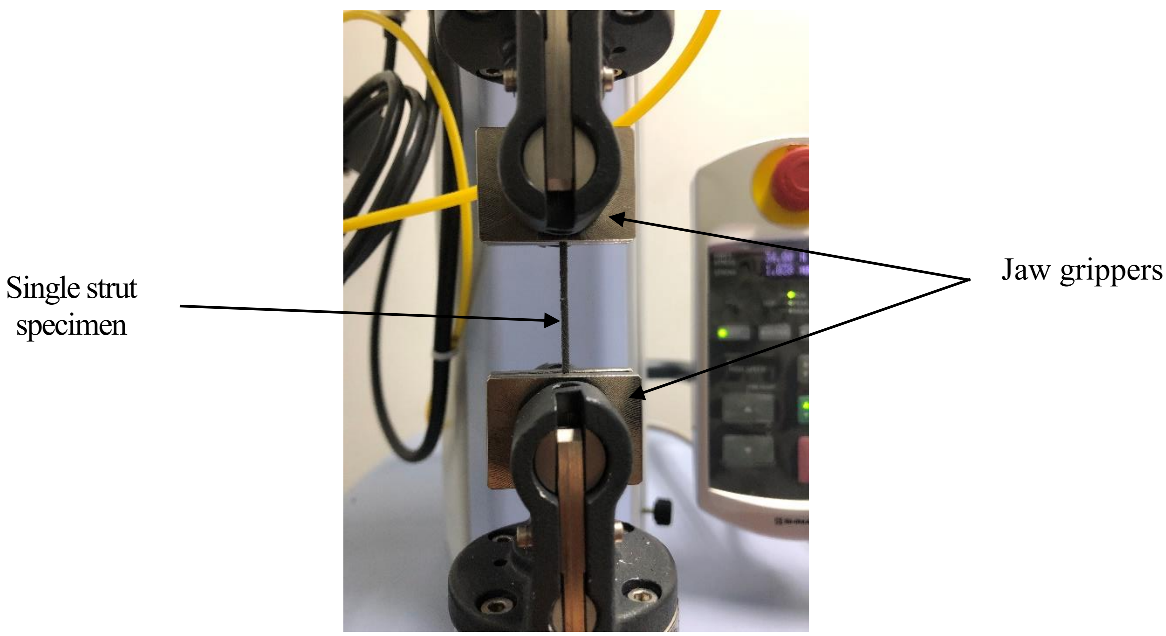

Figure 3.5.2: Tensile tests of the single struts with loading velocity of 0.1 mm/minute by using Shimadzu machine.

3.6 Analysis Stage

In the analysis stage, all data from tensile test are analyzed for each gauge length. The test is repeated 3 times to ensure the accuracy. A table is constructed by the Trapezium software to show the raw data which is load distributed over time for each gauge length. The strain is derived directly from the crosshead displacement and stress can be calculated from force distributed over cross-sectional area of the specimen. Figure 3.6.1 shows the collected and calculated data. Then the stress-strain curve was plotted for each specimen tested. The young's modulus can be obtained from the curve by calculating the gradient using riseover run as shown in Figure 3.6.2.

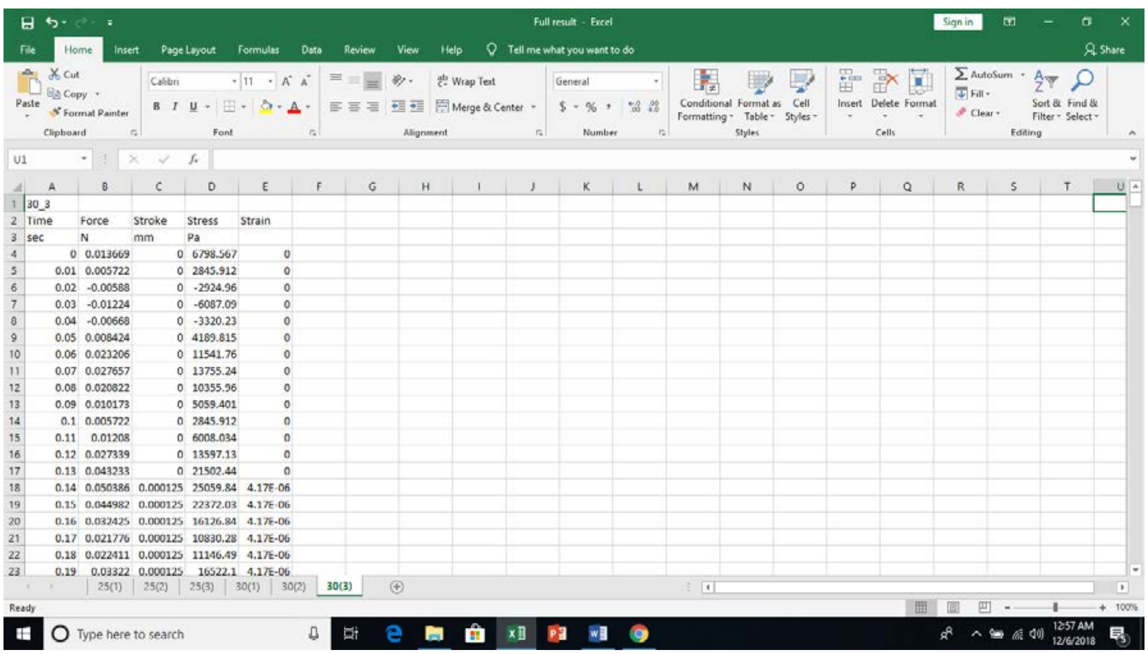

	A	B	C	D	E
1	30_3				
2	Time	Force	Stroke	Stress	Strain
3	sec	N	mm	Pa	
4	0	0.013669	0	6798.567	0
5	0.01	0.005722	0	2845.912	0
6	0.02	-0.00588	0	-2924.96	0
7	0.03	-0.01224	0	-6087.09	0
8	0.04	-0.00668	0	-3320.23	0
9	0.05	0.008424	0	4189.815	0
10	0.06	0.023206	0	11541.76	0
11	0.07	0.027657	0	13755.24	0
12	0.08	0.020822	0	10355.96	0
13	0.09	0.010173	0	5059.401	0
14	0.1	0.005722	0	2845.912	0
15	0.11	0.01208	0	6008.034	0
16	0.12	0.027339	0	13597.13	0
17	0.13	0.043233	0	21502.44	0
18	0.14	0.050386	0.000125	25059.84	4.17E-06
19	0.15	0.044982	0.000125	22372.03	4.17E-06
20	0.16	0.032425	0.000125	16126.84	4.17E-06
21	0.17	0.021776	0.000125	10830.28	4.17E-06
22	0.18	0.022411	0.000125	11146.49	4.17E-06
23	0.19	0.03322	0.000125	16522.1	4.17E-06

Figure 3.6.1: Table of calculated value from a given raw data using Microsoft Excel.

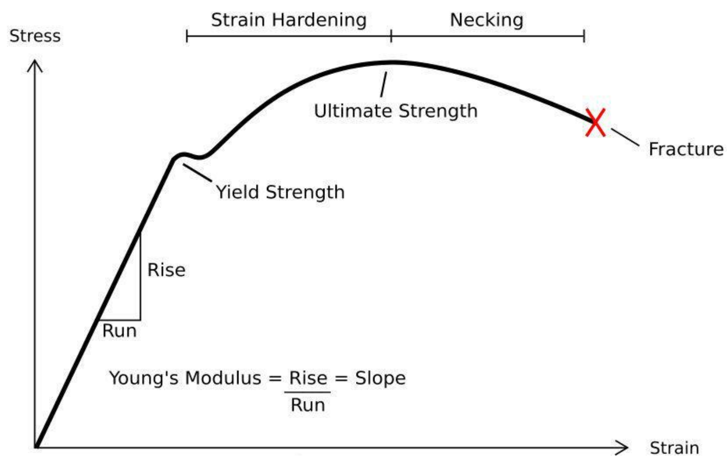

Figure 3.6.2: Young's modulus can be calculated from the stress-strain gradient.

Every specimens data are used to plot the stress-strain curve so as a result three young's modulus for each gauge length are obtained. The average of young's modulus is calculated by using standard deviation to meet the tolerance. From data force, F and total elongation, δ_T another graph was plotted for each gauge length to define the apparent compliance, C_a. Figure 3.6.3 shows the method of finding C_a from force versus elongation plot.

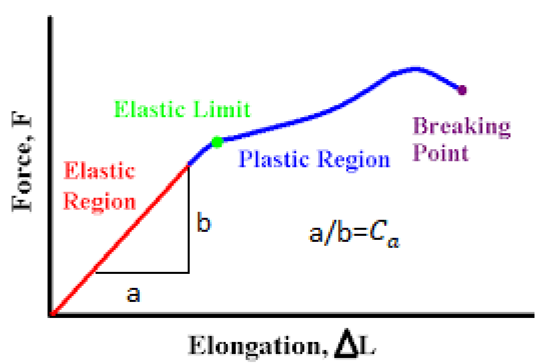

Figure 3.6.3: Extraction of C_a from force versus elongation plotted

Thus, every gauge length has its own C_a and the average values are calculated including the standard deviation. Diameter, D of each specimens after undergoes tensile test were observed by using Dino-lite Pro device. Eight point are observed under the device to find the average of diameter for each specimen. The average diameter of each gauge length then recorded. Plot of C_a versus L/ D^2 are tabulated based on the previous data calculated. Figure 3.6.4 shows the magnification scale of 45x under Dino-lite Pro to measure single struts and Figure 3.6.5 shows the example of plot C_a versus L/ D^2.

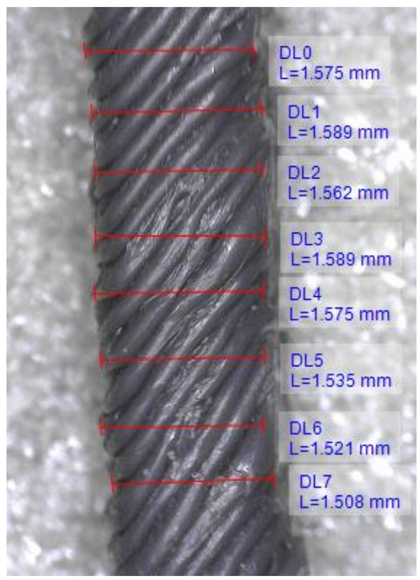

. Figure 3.6.4: The magnification scale of 45 times under Dino-lite Pro to measured single struts.

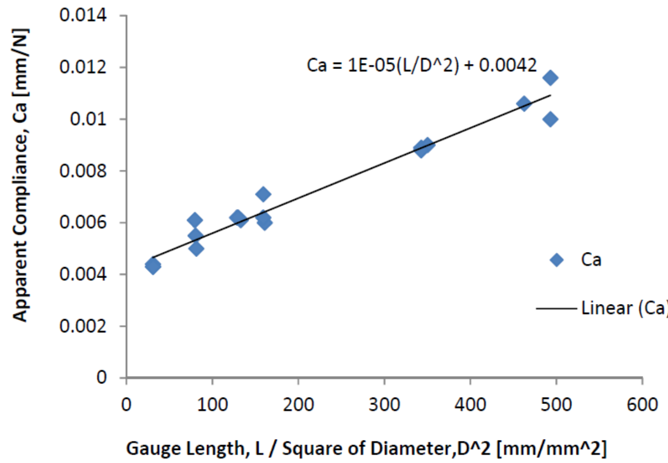

Figure 3.6.5: The example of plot C_a versus L/ D^2.

(source: Hasan, 2013)

Next, compliance correction method is applied to get the accurate result by defining the corrected young's modulus. The fundamental concept behind this method is based on the assumption that the specimen and testing fixture can be modelled as a system with two spring in series. The total measured displacement can be taken as the sum of the displacement in the specimen and the loading system when it is subjected to an equal applied load *F*. Equation 3.6.1 represents the following assumption.

$$\delta_T = \delta_S + \delta_C \qquad \text{(Eq 3.6.1)}$$

δ_T is the total measured displacement and δ_S is the specimen deformation, while δ_C is the displacement in the loading system or known as the machine compliance factor. The apparent compliance factor, C_a can be shown as (C_a = δ_T/*F)* if both specimen and the loading system are assumed as linear springs which related to the machine compliance factor, C_m (= δ_C/*F*) as given in Equation 3.6.2

$$C_a = C_m + (1/EA)\mathrm{L} \qquad \text{(Eq 3.6.2)}$$

A is the cross-sectional area, *L* is the length specimen and *E* is the elastic modulus of the tested specimen. From the ASTM standard, C_m is the zero gauge length intercept on a plotted of C_a versus *L* for a given material where the corrected young's modulus *E* of the material can be obtained from the slope of this plot or calculated from Equation 3.6.4. E_u is the uncorrected elastic modulus of the tested material from Equation 3.6.3 which is initially defined from formula of deformation, (δ = PL/EA).

$$\frac{L}{A} = \frac{\delta_T}{F}\,\mathrm{E} = E_u C_a \qquad \text{(Eq 3.6.3)}$$

$$E = \frac{(\frac{L}{A})}{C_{a-}\,C_m} = \frac{E_u\,C_a}{C_{a-}\,C_m} \qquad \text{(Eq 3.6.4)}$$

Based on the equation 3.6.5 which is modified from Equation 3.6.2, the accurate version of compliance correction method can be obtained. C_m is the zero gauge length intercept on a plot of C_a versus L/D^2 where D is the diameter of the specimen from the area, A ($=\frac{\pi D^2}{4}$) (Li and Langley, 1985).

$$C_a = C_m + (4/\pi E)(L/D^2) \quad \text{(Eq 3.6.5)}$$

The average corrected of young's modulus, E is calculated from equation 3.6.4 where the C_m can be determined by the best line of y-axis intercept on C_a versus L/D^2 plot. When all the data are collected completely, a table of corrected elastic modulus values for different gauge lengths of tensile test result for the single strut are constructed. Example of the table from other study is shown in Figure 3.6.6.

Gauge length [mm]	Average diameter [mm]	Average apparent compliance for test [mm/N]	Average uncorrected E value [GPa]	Average corrected E value [GPa]
30	0.374 ± 0.007	0.0107 ± 0.0008	27 ± 1.9	44 ± 5.2
22	0.379 ± 0.002	0.0089 ± 0.0001	24 ± 0.3	45 ± 0.9
10	0.375 ± 0.001	0.0064 ± 0.0006	17 ± 1.7	50 ± 12
8	0.371 ± 0.003	0.0062 ± 0.00006	14 ± 0.6	43 ± 1.7
5	0.374 ± 0.002	0.0055 ± 0.0006	10 ± 1.9	45 ± 21
	0.375 ± 0.004		Ave. E from all gauge lengths	45 ± 9.9

Figure 3.6.6: The example of corrected elastic modulus values for different gauge lengths of tensile test result for the single struts table

(source: Hasan, 2013)

3.7 Conclusion of Chapter 3

The purpose of creating methodology is to plan all activities in order to accomplish this study. A well-prepared strategy is arranged to conduct all activities efficiently. All result from this chapter will be discussed in detail on the next chapter.

CHAPTER 4

RESULT AND DISCUSSION

4.1 Introduction

In this chapter, all the result and data obtained from the study will be discussed. The basic theoretical in calculating the result is explained clearly to lead this study complete.

4.2 Characterization of single strut

For the characterization of single strut, Figure 4.2.1 (a), (b) and (c) shows a single strut is placed under microscope which is Dino-Lite Pro to measure its post test diameter. The diameter have been calculated as an average 1.6 mm.

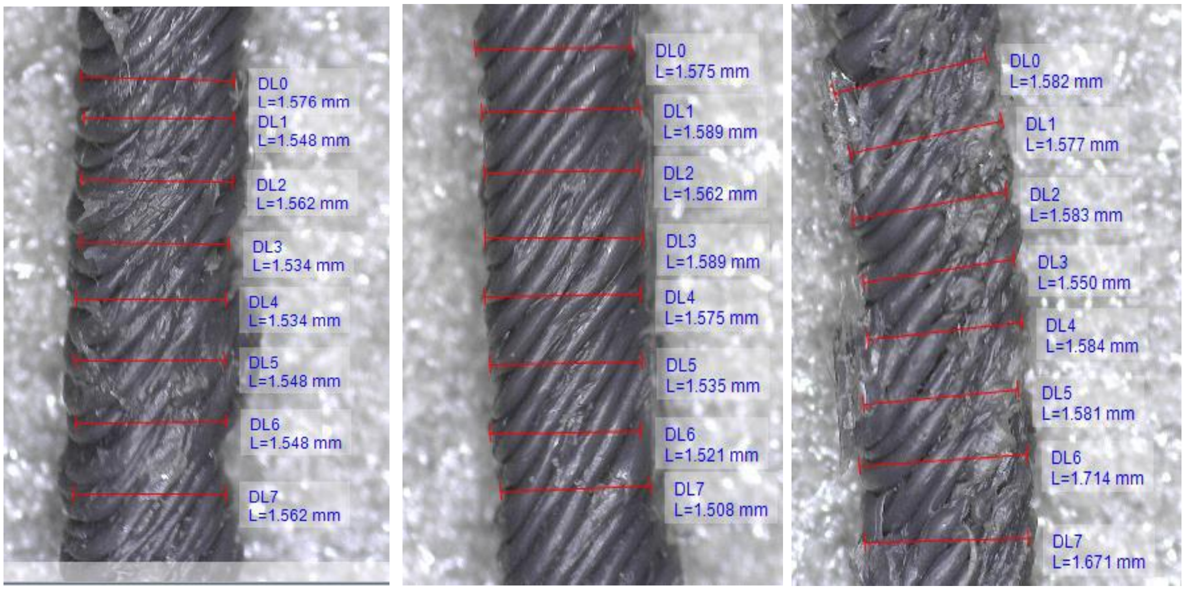

Figure 4.2.1: Determination of diameter on single struts using Dino-Lite Pro at 45 times magnification.

4.3 Elastic modulus, *E*

From the raw data given by the tensile test, stress-strain curve is constructed for each specimens. The modulus of elasticity was determined by calculating the gradient of the best line on each graph. All are shown in Table 4.3.1 until Table 4.3.5. The Figure 4.3.1 show the elastic modulus, *E* at several gauge length, between 0.03 m to 0.003 m.

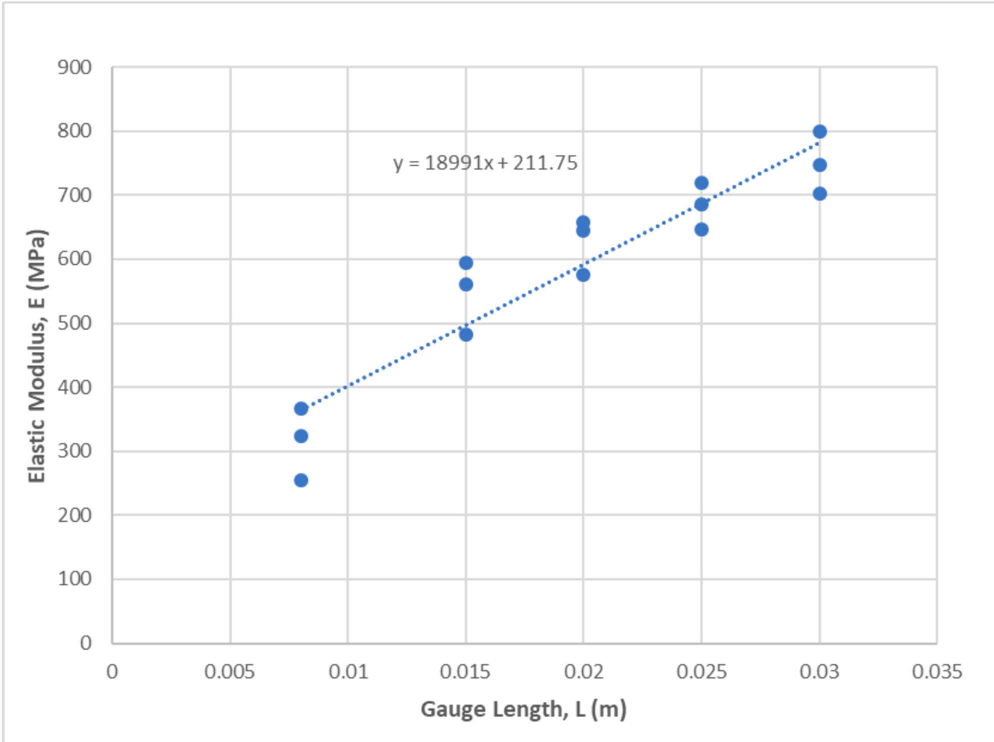

Figure 4.3.1: Plot of elastic modulus versus gauge length.

Table 4.3.1: The elastic modulus, E for 30 mm gauge length specimens.

Gauge length= 30 mm	Stress versus Strain	Elastic modulus, *E* (MPa)
Specimen 1	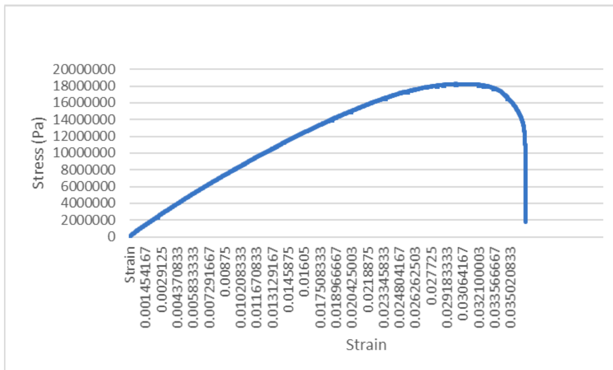	798.679
Specimen 2	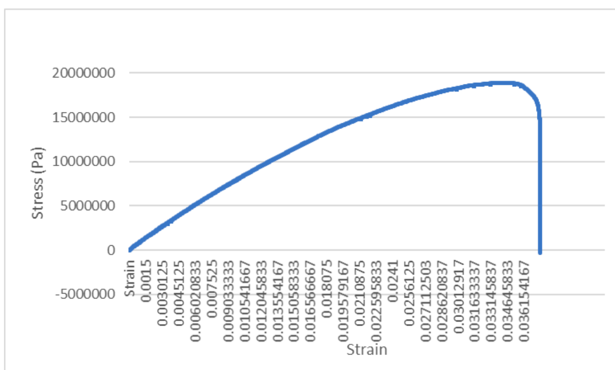	746.733
Specimen 3	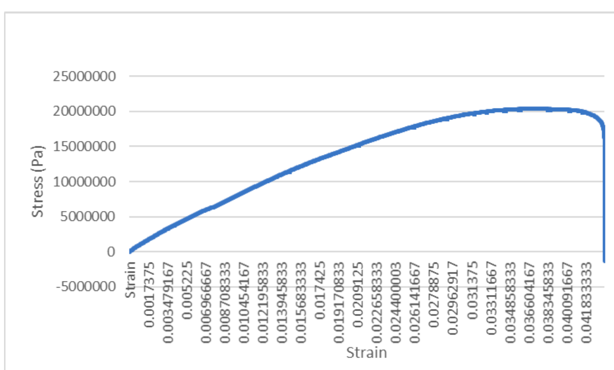	702.576

Table 4.3.2: The elastic modulus, E for 25 mm gauge length specimens.

<table>
<tr><th>Gauge length= 25 mm</th><th>Stress versus Strain</th><th>Elastic modulus , E (MPa)</th></tr>
<tr><td>Specimen 1</td><td>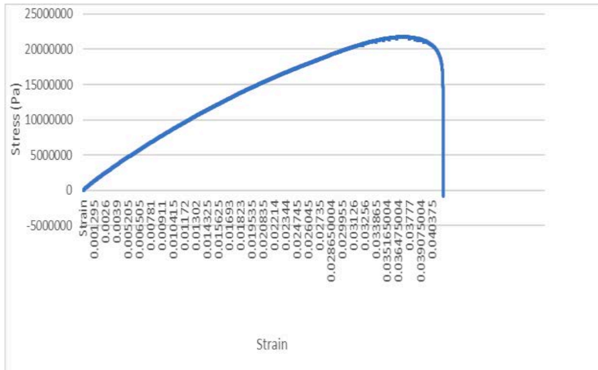
</td><td>719.942</td></tr>
<tr><td>Specimen 2</td><td>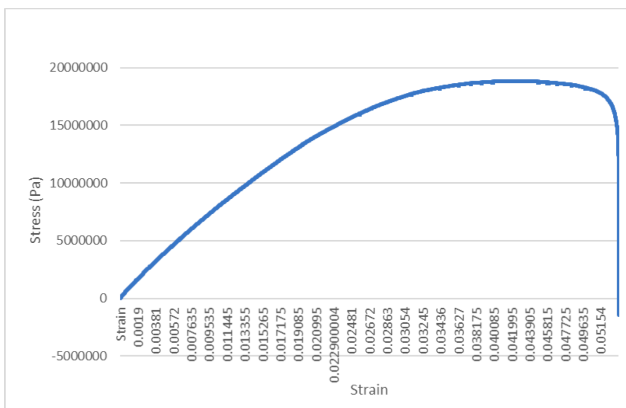
</td><td>685.401</td></tr>
<tr><td>Specimen 3</td><td>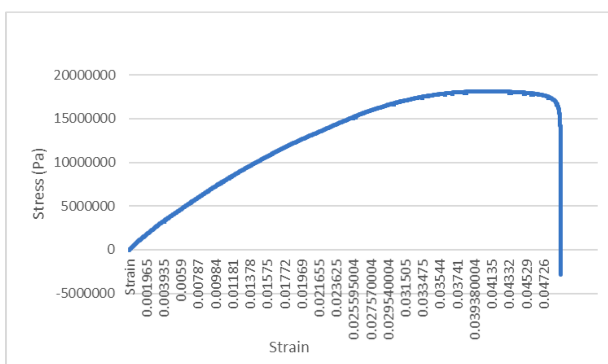
</td><td>647.249</td></tr>
</table>

Table 4.3.3: The elastic modulus, E for 20 mm gauge length specimens.

<table>
<tr><th>Gauge length= 20 mm</th><th>Stress versus Strain</th><th>Elastic modulus , E (MPa)</th></tr>
<tr><td>Specimen 1</td><td>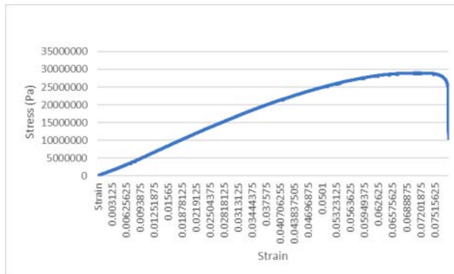
</td><td>574.713</td></tr>
<tr><td>Specimen 2</td><td>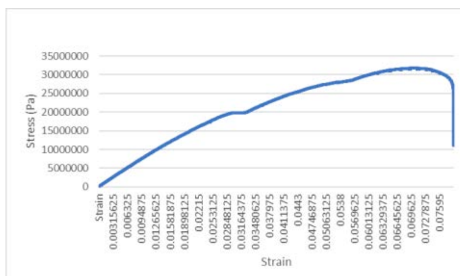
</td><td>657.354</td></tr>
<tr><td>Specimen 3</td><td>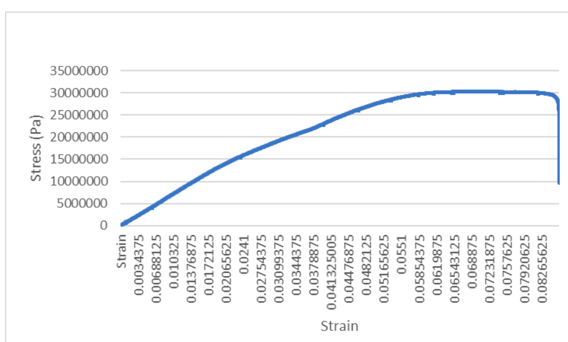
</td><td>643.863</td></tr>
</table>

Table 4.3.4: The elastic modulus. E for 15 mm gauge length specimens.

Gauge length= 15 mm	Stress versus Strain	Elastic modulus, E (MPa)
Specimen 1	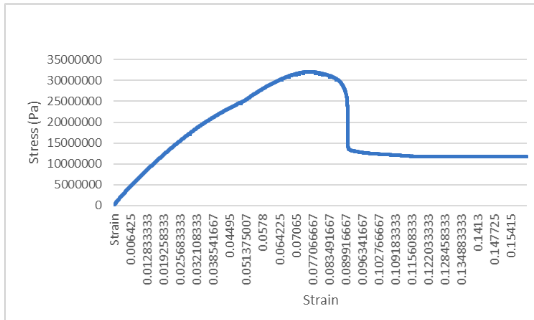	560.486
Specimen 2	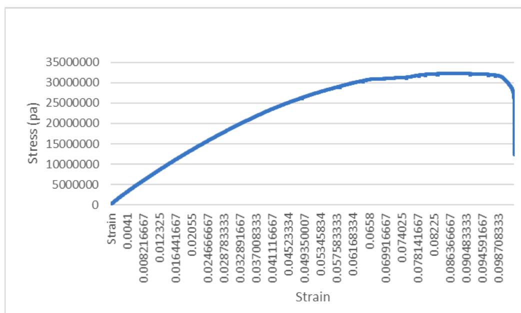	593.765
Specimen 3	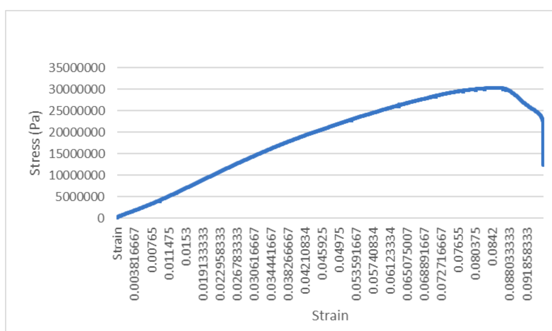	482.121

Table 4.3.5: The elastic modulus, E for 8 mm gauge length specimens.

Gauge length= 8 mm	**Stress versus Strain**	**Elastic modulus, E (MPa)**
Specimen 1	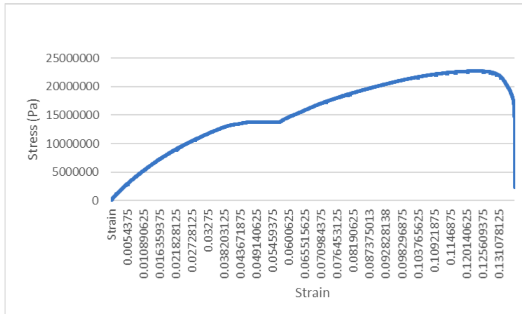	324.544
Specimen 2	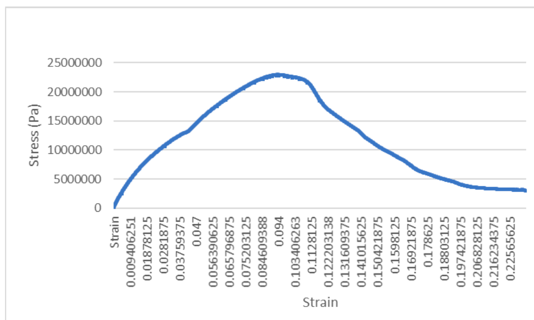	255.183
Specimen 3	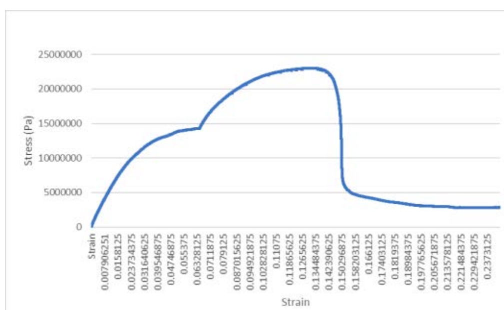	366.973

4.4 Apparent compliance factor, C_a.

From force versus elongation curve, the apparent compliance for each specimens are extracted as shown in table 4.4.1 until table 4.4.5.

Table 4.4.1: The apparent compliance, Ca for 30 mm gauge length specimens.

Gauge length= 30 mm	**Force versus elongation**	**Apparent compliance, C_a(m/N)**
Specimen 1	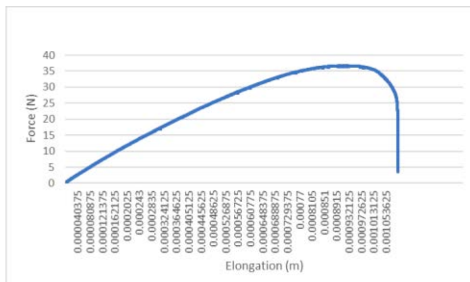	1.779×10^{-5}
Specimen 2	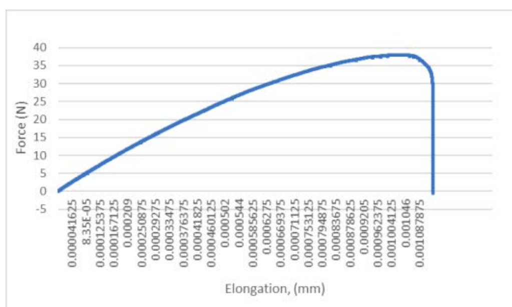	1.885×10^{-5}
Specimen 3	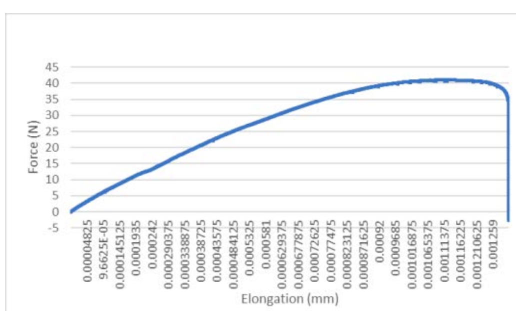	1.963×10^{-5}

Table 4.4.2: The apparent compliance, C_a for 25 mm gauge length specimens.

Gauge length= 25 mm	**Force versus elongation**	**Apparent compliance, C_a(m/N)**
Specimen 1	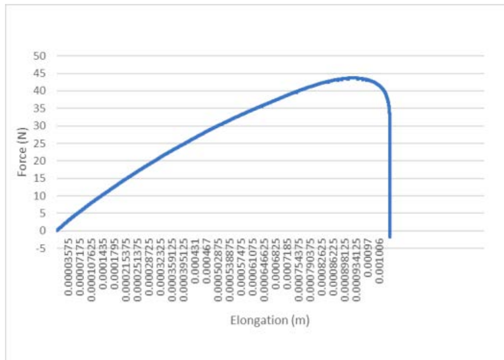	$1.638{\times}10^{-5}$
Specimen 2	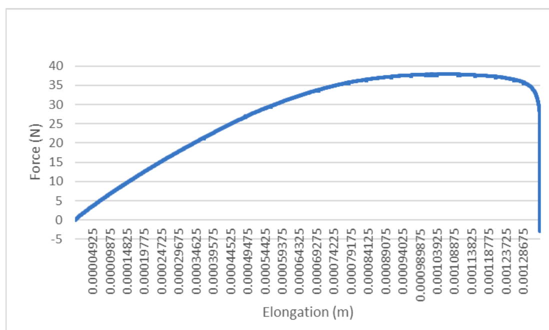	$1.744{\times}10^{-5}$
Specimen 3	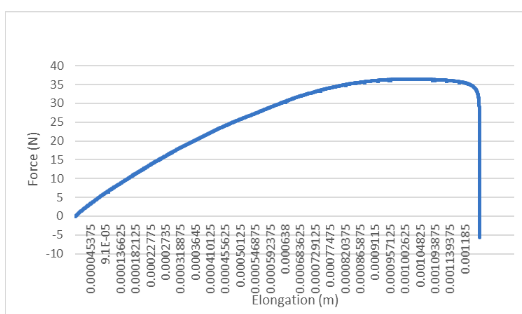	$1.848{\times}10^{-5}$

Table 4.4.3: The apparent compliance, C_a for 20 mm gauge length specimens.

Gauge length= 20 mm	**Force versus elongation**	**Apparent compliance, C_a(m/N)**
Specimen 1	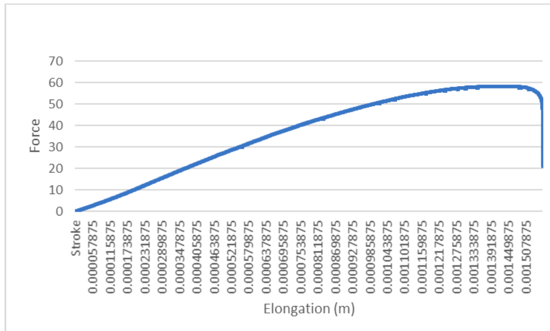	1.678×10^{-5}
Specimen 2	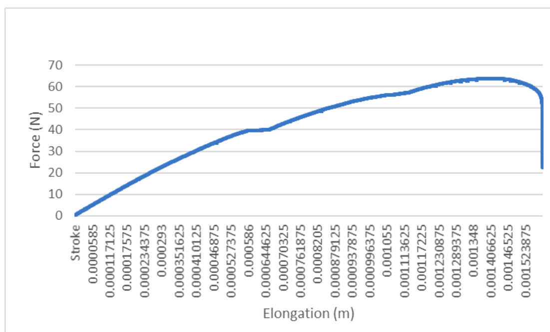	1.250×10^{-5}
Specimen 3	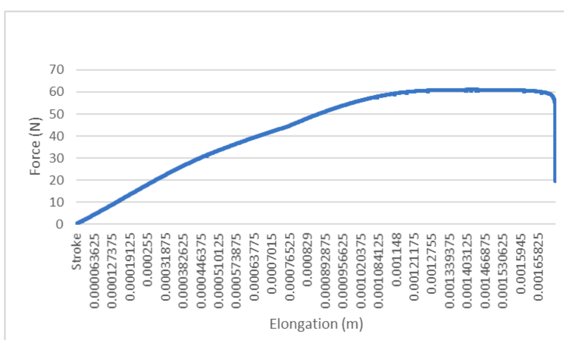	1.470×10^{-5}

Table 4.4.3: The apparent compliance, C_a for 15 mm gauge length specimens.

<table>
<tr><th>Gauge length= 15 mm</th><th>Force versus elongation</th><th>Apparent compliance, C_a(m/N)</th></tr>
<tr><td>Specimen 1</td><td>
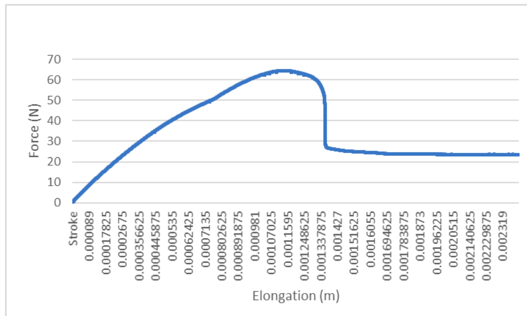

</td><td>1.161×10^{-5}</td></tr>
<tr><td>Specimen 2</td><td>
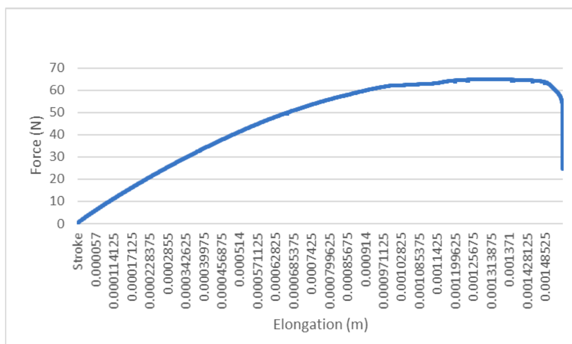

</td><td>1.165×10^{-5}</td></tr>
<tr><td>Specimen 3</td><td>
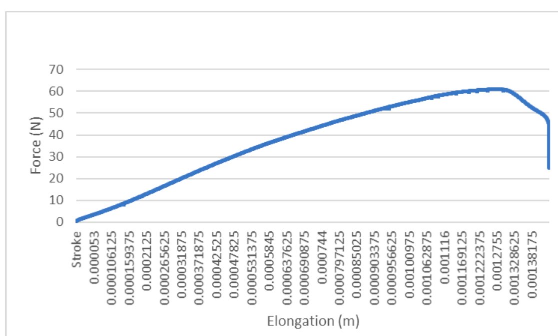

</td><td>1.539×10^{-5}</td></tr>
</table>

Table 4.4.5: The apparent compliance, C_a for 8 mm gauge length specimens.

Gauge length= 8 mm	**Force versus elongation**	**Apparent compliance, C_a(m/N)**
Specimen 1	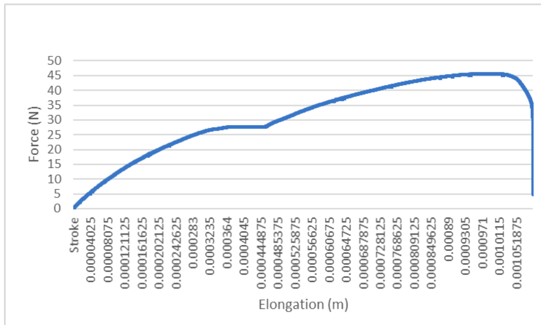	7.775×10^{-6}
Specimen 2	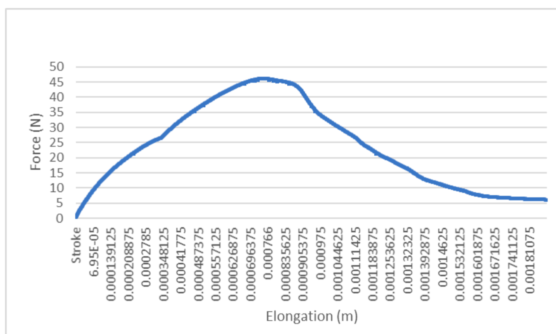	1.025×10^{-5}
Specimen 3	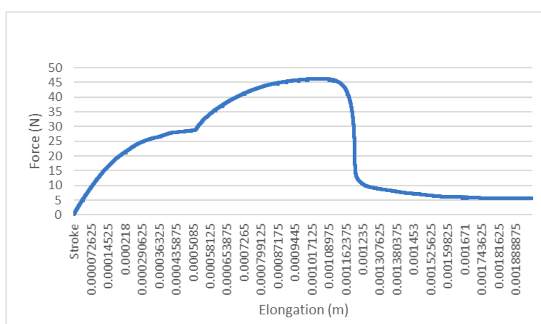	9.000×10^{-6}

4.5 Machine compliance factor, C_m

A scatter chart is plotted which is apparent compliance, C_a versus length, l over square of diameter, *D.* A trendline was constructed on this scatter plot and the machine compliance factor, C_m are extracted from the y-intercept which is 6×10^{-6}. The graph and the linear equation of the trendline are shown in Figure 4.5.1.

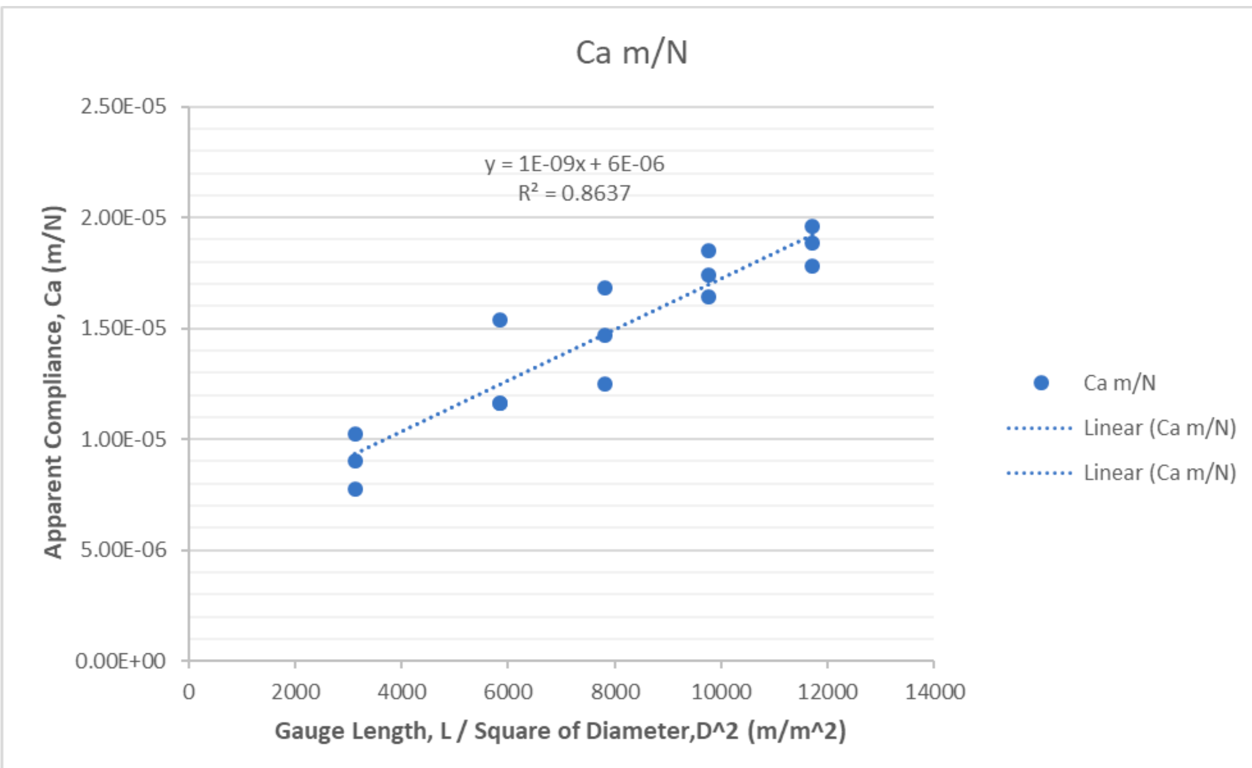

Figure 4.5.1: Graph of apparent compliance, C_a versus length, l over square of diameter, *D* with the linear equation of the trendline.

4.6 Calculated result

After all the data have been calculated, a table is constructed to shown the final result. The gauge length, average diameter, average compliance factor, average uncorrected and uncorrected modulus of elasticity was recorded as shown in Table 4.6.1.

Table 4.6.1: List of corrected elastic modulus values for different gauge lengths of tensile test result for the ABS single-struts (The ± values are from standard deviation values of each repetition)

Gauge length, *l* (mm)	**Average diameter, *D* (m)**	**Average compliance, C_a for test (m/N)**	**Average uncorrected modulus of elasticity, E (MPa)**	**Average corrected modulus of elasticity, E (MPa)**
30	0.0016	$1.875\times10^{-5} \pm 9.235\times10^{-7}$	749.329 ± 48.104	1120.636 ± 74.880
25	0.0016	$1.743\times10^{-5} \pm 1.050\times10^{-6}$	684.197 ± 36.361	1049.097 ± 87.632
20	0.0016	$1.466\times10^{-5} \pm 2.140\times10^{-6}$	625.310 ± 44.334	1082.113 ± 185.019
15	0.0016	$1.288\times10^{-5} \pm 2.171\times10^{-6}$	545.457 ± 57.319	1058.107 ± 234.252
8	0.0016	$9.008\times10^{-6} \pm 1.238\times10^{-6}$	315.567 ± 56.433	1045.925 ± 405.792
Average modulus of elasticity, *E* from all gauge length				1071.176 ± 31.072

Calculation for 30 mm gauge length specimens

Specimen 1

E_u = 798.669 MPa, C_a = 1.779 $\times 10^{-5}$ m/N, C_m = 6 $\times 10^{-6}$

From Equation 3.6.4

$$E = \frac{(\frac{L}{A})}{C_{a-}\ C_m} = \frac{E_u\ C_a}{C_{a-}\ C_m}$$

E = (798.669 MPa × 1.779 $\times 10^{-5}$ m/N) / (1.779 $\times 10^{-5}$ m/N - 6 × 10^{-6}) = 1204.411 MPa

Specimen 2

E_u = 746.733 MPa, C_a = 1.885 $\times 10^{-5}$ m/N, C_m = 6 $\times 10^{-6}$

$$E = \frac{(\frac{L}{A})}{C_{a-}\ C_m} = \frac{E_u\ C_a}{C_{a-}\ C_m}$$

E = (746.733 MPa × 1.885 $\times 10^{-5}$ m/N) / (1.885 $\times 10^{-5}$ m/N - 6 × 10^{-6}) = 1097.276 MPa

Specimen 3

E_u = 702.576 MPa, C_a = 1.779 $\times 10^{-5}$ m/N, C_m = 6 $\times 10^{-6}$

$$E = \frac{(\frac{L}{A})}{C_{a-}\ C_m} = \frac{E_u\ C_a}{C_{a-}\ C_m}$$

E = (702.576 MPa × 1.779 $\times 10^{-5}$ m/N) / (1.779 $\times 10^{-5}$ m/N - 6 × 10^{-6}) = 1060.221 MPa

Average E

$\bar{x}$ = (1204.411 MPa + 1097.276 MPa + 1060.221 MPa) / 3 = 1120.636 MPa

with standard deviation, σ = ± 74.880

<u>Calculation for 25 mm gauge length specimens</u>

<u>Specimen 1</u>

E_u = 719.942 MPa, C_a = 1.638 ×10^{-5} m/N, C_m = 6 × 10^{-6}

From Equation 3.6.4

$$E = \frac{(\frac{L}{A})}{C_{a-}\,C_m} = \frac{E_u\,C_a}{C_{a-}\,C_m}$$

E = (719.942 MPa × 1.638 ×10^{-5} m/N) / (1.638 ×10^{-5} m/N - 6 × 10^{-6}) = 1136.802 MPa

<u>Specimen 2</u>

E_u = 685.400 MPa, C_a = 1.744 ×10^{-5} m/N, C_m = 6 × 10^{-6}

$$E = \frac{(\frac{L}{A})}{C_{a-}\,C_m} = \frac{E_u\,C_a}{C_{a-}\,C_m}$$

E = (685.400 MPa × 1.744 ×10^{-5} m/N) / (1.744 ×10^{-5} m/N - 6 × 10^{-6}) = 1048.951 MPa

<u>Specimen 3</u>

E_u = 647.249 MPa, C_a = 1.848 ×10^{-5} m/N, C_m = 6 × 10^{-6}

$$E = \frac{(\frac{L}{A})}{C_{a-}\,C_m} = \frac{E_u\,C_a}{C_{a-}\,C_m}$$

E = (647.249 MPa × 1.848 ×10^{-5} m/N) / 1.848 ×10^{-5} m/N - 6 × 10^{-6}) = 961.538 MPa

<u>Average E</u>

$\bar{x}$ = (1136.802 MPa + 1048.951 MPa + 961.538 MPa) / 3 = 1049.097 MPa

with standard deviation, σ = ± 87.632

Calculation for 20 mm gauge length specimens

Specimen 1

E_u = 574.713 MPa, C_a = 1.679 ×10^{-5} m/N, C_m = 6 × 10^{-6}

From Equation 3.6.4

$$E = \frac{(\frac{L}{A})}{C_{a-}\,C_m} = \frac{E_u\,C_a}{C_{a-}\,C_m}$$

E = (574.713 MPa × 1.679 ×10^{-5} m/N) / (1.679 ×10^{-5} m/N - 6 × 10^{-6}) = 894.254 MPa

Specimen 2

E_u = 657.354 MPa, C_a = 1.250 ×10^{-5} m/N, C_m = 6 × 10^{-6}

$$E = \frac{(\frac{L}{A})}{C_{a-}\,C_m} = \frac{E_u\,C_a}{C_{a-}\,C_m}$$

E = (657.354 MPa × 1.250 ×10^{-5} m/N) / (1.250 ×10^{-5} m/N - 6 × 10^{-6}) = 1264.154 MPa

Specimen 3

E_u = 643.863 MPa, C_a = 1.470 ×10^{-5} m/N, C_m = 6 × 10^{-6}

$$E = \frac{(\frac{L}{A})}{C_{a-}\,C_m} = \frac{E_u\,C_a}{C_{a-}\,C_m}$$

E = (643.863 MPa × 1.470 ×10^{-5}m/N) / 1.470 ×10^{-5} m/N - 6 × 10^{-6}) = 1087.931 MPa

Average E

$\bar{x}$ = (894.254 MPa + 1264.154 MPa + 1087.931 MPa) / 3 = 1082.113 MPa

with standard deviation, σ = ± 185.019

Calculation for 15 mm gauge length specimens

Specimen 1

E_u = 560.486 MPa, C_a = 1.161 ×10^{-5} m/N, C_m = 6 × 10^{-6}

From Equation 3.6.4

$$E = \frac{(\frac{L}{A})}{C_{a-}\ C_m} = \frac{E_u\ C_a}{C_{a-}\ C_m}$$

E = (560.486 MPa × 1.161 ×10^{-5} m/N) / (1.161 ×10^{-5} m/N - 6 × 10^{-6}) = 1159.893 MPa

Specimen 2

E_u = 593.765 MPa, C_a = 1.165 ×10^{-5} m/N, C_m = 6 × 10^{-6}

$$E = \frac{(\frac{L}{A})}{C_{a-}\ C_m} = \frac{E_u\ C_a}{C_{a-}\ C_m}$$

E = (593.765 MPa × 1.165 ×10^{-5} m/N) / (1.165 ×10^{-5} m/N - 6 × 10^{-6}) = 1224.248 MPa

Specimen 3

E_u = 482.121 MPa, C_a = 1.539 ×10^{-5} m/N, C_m = 6 × 10^{-6}

$$E = \frac{(\frac{L}{A})}{C_{a-}\ C_m} = \frac{E_u\ C_a}{C_{a-}\ C_m}$$

E = (482.121 MPa × 1.539 ×10^{-5}m/N) / 1.539 ×10^{-5} m/N - 6 × 10^{-6}) = 790.181 MPa

Average E

$\bar{x}$ = (1159.893 MPa + 1224.248 MPa + 790.181 MPa) / 3 = 1058.107 MPa

with standard deviation, σ = ± 234.252

Calculation for 8 mm gauge length specimens

Specimen 1

E_u = 324.544 MPa, C_a = 7.775 ×10^{-6} m/N, C_m = 6 × 10^{-6}

From Equation 3.6.4

$$E = \frac{(\frac{L}{A})}{C_{a-} C_m} = \frac{E_u \, C_a}{C_{a-} C_m}$$

E = (324.544 MPa × 7.775 ×10^{-6} m/N) / (7.775 ×10^{-6} m/N - 6 × 10^{-6}) = 1421.408 MPa

Specimen 2

E_u = 255.183 MPa, C_a = 1.025 ×10^{-5} m/N, C_m = 6 × 10^{-6}

$$E = \frac{(\frac{L}{A})}{C_{a-} C_m} = \frac{E_u \, C_a}{C_{a-} C_m}$$

E = (255.183 MPa × 1.025 ×10^{-5} m/N) / (1.025 ×10^{-5} m/N - 6 × 10^{-6}) = 615.435 MPa

Specimen 3

E_u = 366.973 MPa, C_a = 9.000 ×10^{-6} m/N, C_m = 6 × 10^{-6}

$$E = \frac{(\frac{L}{A})}{C_{a-} C_m} = \frac{E_u \, C_a}{C_{a-} C_m}$$

E = (366.973 MPa × 9.000 ×10^{-6}m/N) / (9.000 ×10^{-6} m/N - 6 × 10^{-6}) = 1100.933 MPa

Average E

$\bar{x}$ = (1421.408 MPa + 615.435 MPa + 1100.933 MPa) / 3 = 1045.925 MPa

with standard deviation, σ = ± 405.792

Based on the result obtained, the slope from the graph shown that the tensile test on single strut ran in correct method alike to the other study related, (Hasan,2013). The failure point on all single struts are still in between the gauge length. As compared the stress-strain plot between all gauge length, its shows the shorter the gauge length so the higher the distribution of force needed in the tensile test. Young's modulus directly calculated from gradient of stress-strain plot as the corrected young's modulus need to be defined to accomplish this study. The apparent compliance, C_a can be determine from graph force versus elongation which the method are shown in previous section. After the tensile test have been done, the post test diameter of single strut need to be determine for the further calculation. C_m was determined from the y-intercept of graph of apparent compliance, C_a versus length, l over square of diameter, *D*. The corrected elastic modulus was calculated from Equation 3.6.4. All the data were calculated as an average value by using standard deviation method and recorded on the Table 4.6.1.

For all gauge length that have been tested, the curve of strain versus stress and force versus elongation were calculated without any error except for the specimen with 8 mm gauge length. Refer to Table 4.3.5 and Table 4.4.5 for 8 mm gauge length, there is uneven curve produced which is cause by slippery of specimens with the jaw gripper of the tensile machine. This slippery happened on the 8 mm specimens only because of the part of the specimens which the jaw gripper hold during the testing was the shortest among the others specimens which is 8 mm on the top and above the gauge length. Accordingly to the case, the resistance force to hold the specimens were unsufficient while the jaw gripper pull the specimens in parallel. However the data collected from the graph which is the young modulus and apparent compliance, C_a are calculated before the slippery occur to make sure the precision of final data.

Table 4.6.1 is constructed to show the final data produced. Every specimens with different gauge length have different values of uncorrected elastic modulus and this proved that high dependency of elastic modulus for single strut on the gauge length. Compliance correction method is applied in order to produce the corrected elastic modulus by removing the machine compliance factor, C_m from the whole system.

Corrected elastic modulus, the values collected are within small variation and the range is from 1045.925 MPa to 1120.636 MPa which produce the average value of 1071.176 MPa. All the values calculated for each gauge length were between the standard value of ABS elastic modulus as shown in figure 4.6.1 which is from 1.0 GPa to 2.65 GPa.

Mechanical Properties	Metric	English	Comments
Hardness, Rockwell R	68.0 - 113	68.0 - 113	Average value: 101 Grade Count:63
Ball Indentation Hardness	65.0 - 110 MPa	9430 - 16000 psi	Average value: 93.2 MPa Grade Count:11
Tensile Strength, Ultimate	22.1 - 49.0 MPa	3210 - 7110 psi	Average value: 36.4 MPa Grade Count:31
Tensile Strength, Yield	13.0 - 65.0 MPa	1890 - 9430 psi	Average value: 40.5 MPa Grade Count:117
	22.1 - 59.3 MPa @Temperature -18.0 - 71.0 °C	3210 - 8600 psi @Temperature -0.400 - 160 °F	Average value: 40.7 MPa Grade Count:1
Elongation at Break	3.00 - 150 %	3.00 - 150 %	Average value: 34.2 % Grade Count:71
Elongation at Yield	0.620 - 30.0 %	0.620 - 30.0 %	Average value: 5.57 % Grade Count:49
Modulus of Elasticity	1.00 - 2.65 GPa	145 - 384 ksi	Average value: 2.07 GPa Grade Count:57
	1.50 - 2.60 GPa @Temperature -18.0 - 71.0 °C	218 - 377 ksi @Temperature -0.400 - 160 °F	Average value: 2.05 GPa Grade Count:1
Flexural Yield Strength	0.379 - 593 MPa	55.0 - 86000 psi	Average value: 69.2 MPa Grade Count:78
	49.6 - 113.8 MPa @Temperature -40.0 - 71.0 °C	7190 - 16510 psi @Temperature -40.0 - 160 °F	Average value: 81.7 MPa Grade Count:1
Flexural Modulus	0.200 - 5.50 GPa	29.0 - 798 ksi	Average value: 2.20 GPa Grade Count:105
	1.90 - 2.80 GPa @Temperature -40.0 - 71.0 °C	276 - 406 ksi @Temperature -40.0 - 160 °F	Average value: 2.35 GPa Grade Count:1
Izod Impact, Notched	0.380 - 10.3 J/cm	0.712 - 19.3 ft-lb/in	Average value: 3.22 J/cm Grade Count:88
	0.450 - 4.00425 J/cm @Temperature -40.0 - 0.000 °C	0.843 - 7.50160 ft-lb/in @Temperature -40.0 - 32.0 °F	Average value: 1.34 J/cm Grade Count:21
	0.480 - 4.00 J/cm @Temperature -40.0 - 0.000 °C	0.899 - 7.49 ft-lb/in @Temperature -40.0 - 32.0 °F	Average value: 1.34 J/cm Grade Count:12
	0.480 - 4.00 J/cm @Thickness 3.17 - 6.40 mm	0.899 - 7.49 ft-lb/in @Thickness 0.125 - 0.252 in	Average value: 1.34 J/cm Grade Count:12
Izod Impact, Unnotched	1.07873 - 1.66713 J/cm @Temperature -20.0 - -20.0 °C	2.02091 - 3.12322 ft-lb/in @Temperature -4.00 - -4.00 °F	Average value: 1.37 J/cm Grade Count:2
	1.07873 - 1.66713 J/cm @Thickness 3.20 - 6.40 mm	2.02091 - 3.12322 ft-lb/in @Thickness 0.126 - 0.252 in	Average value: 1.37 J/cm Grade Count:2
Izod Impact, Notched (ISO)	8.00 - 42.0 kJ/m²	3.81 - 20.0 ft-lb/in²	Average value: 26.4 kJ/m² Grade Count:24
	7.00 - 22.0 kJ/m² @Temperature -30.0 - -20.0 °C	3.33 - 10.5 ft-lb/in² @Temperature -22.0 - -4.00 °F	Average value: 13.0 kJ/m² Grade Count:15
	7.00 - 7.00 kJ/m² @Temperature -40.0 - -40.0 °C	3.33 - 3.33 ft-lb/in² @Temperature -40.0 - -40.0 °F	Average value: 13.0 kJ/m² Grade Count:1
	7.00 - 7.00 kJ/m² @Thickness 4.00 - 4.00 mm	3.33 - 3.33 ft-lb/in² @Thickness 0.157 - 0.157 in	Average value: 13.0 kJ/m² Grade Count:1
Charpy Impact Unnotched	11.0 J/cm² - NB	52.4 ft-lb/in² - NB	Average value: 15.4 J/cm² Grade Count:19
	1.00 J/cm² - NB @Temperature -40.0 - -30.0 °C	4.76 ft-lb/in² - NB @Temperature -40.0 - -22.0 °F	Average value: 8.56 J/cm² Grade Count:20
Charpy Impact, Notched	0.700 - 5.00 J/cm²	3.33 - 23.8 ft-lb/in²	Average value: 2.46 J/cm² Grade Count:29
	0.500 - 2.50 J/cm² @Temperature -30.0 - -20.0 °C	2.38 - 11.9 ft-lb/in² @Temperature -22.0 - -4.00 °F	Average value: 1.43 J/cm² Grade Count:18
Dart Drop, Total Energy	24.4 - 50.2 J	18.0 - 37.0 ft-lb	Average value: 31.9 J Grade Count:5
Falling Dart Impact	19.0 - 569 J	14.0 - 420 ft-lb	Average value: 185 J Grade Count:3
Instrumented Impact Total Energy	14.0 - 47.5 J	10.3 - 35.0 ft-lb	Average value: 24.1 J Grade Count:4
Instrumented Impact Energy at Peak	11.0 - 33.9 J	8.11 - 25.0 ft-lb	Average value: 18.8 J Grade Count:3

Figure 4.7.1: Standard material properties of acrylonitrile butadiene styrene, ABS retrieved from www.metwab.com

The value in the range of elastic modulus as shown may affected during the fabrication and testing stage. Single strut was extruded by the 3d printer which various variables were concern in order to find the modulus elasticity of specimen such as the speed of extrusion, temperature on the 3d printer nozzle and pattern selection. For the testing stage, the tensile machine need to be precise with minimum value of errors. The single strut also need to be installed on the jaw gripper properly to avoid sliding during the testing. Every single details as mentioned may affected the result in this experiment.

4.7 Summary of chapter 4

In conclusion, all specimens with different gauge length were succesfully printed by using CubePro. In order to produce identical properties of single struts, all settings used were permanent for every extrusion of CubePro. Next, the single strus are tested on a tensile test machine using shimadzhu and result obatined are tabulated. Compliance correction method is applied to produced the corrected elastic modulus for each specimens and will be compared with the standard value of ABS.

CHAPTER 5

CONCLUSION AND RECOMMENDATION

5.1 Conclusion

This study is conducted to investigate mechanical properties of 3D printed single strut with different gauge length using Shimadzhu tensile test. The choosen diamaters of single struts are 1.6 mm and the build angle are set 35.26º as it represents the angle of the struts to the surface in BCC structure. For the selected parameter in this study, gauge length of single struts have been designed as 8 mm, 15 mm, 20 mm, 25 mm, and 30 mm which one third of the total length of specimen. The background of this study is reviewed to gain the relevent knowledge and scientific theories of the fabricated single struts. The previous researches are studied to analyse layer by layer formation of fabricated single strut using fused deposition modelling (FDM) machine several parameters.

In methodology, CAD software which is CATIA is used to designed single struts. Next the designed single struts are fabricated using CubePro 3D printer. Dino-Lite Pro is used to determine their diameter before being tested on Shimadzhu table top tensile test. All the raw data are calculated by using compliance correction method to define the final result. By following workflow chart, the results are obtained and discussed in this study.

Five sets of single struts with different length are fabricated using CubePro 3D printer successfully. For the diameter analysis, 1.6 mm is the average diameter obtained through Dino-Lite Pro. The stress versus strain and force versus elongation plot are constructed from the raw data obtained on the tensile test. Corrected elastic modulus is calculated by using compliance correction method which have value between 1045.925 MPa to 1120.636 MPa and the average value is 1071.176 MPa. All the corrected values obtained is between the range of standard value of ABS elastic modulus which is from 1.0 GPa to 2.65 GPa. This conclude that the study is succesfully done and the data obtained is valid between the range of theoretical value. The corrected elastic modulus is choosen as the mechanical properties of the single struts because the values are all within small variations unlike to the uncorrected values which depending on the gauge length.

5.2 Recommendation

Through the parameters of gauge length that have undergoes tensile test, all the standard deviations were low which suggesting that data was consistent and that the testing procedure was valid and repeatable. In technically, the single struts not slippered form jaws grip of the Shimadzhu tensile test machine but for the shorter gauge length which is at 8 mm gauge length there is some error occured. This is because, the shorter the gauge length of specimen, the higher the force that need to distribute in the tensile test and this cause the specimen slipped form the jaw grip.

One of the opinion to solved this error is to put a double sided tape or the highest grid sand paper on the jaws grip to avoid slippery of specimens during the test. During the fabrication stage, the printed single struts need to separate from its support intensively. A defect on surface of the struts will effect the data on tensile test as the diemeter is not constant throughout the body. For the future study, factor on fabrication and design method on mechanical properties of single struts can be conducted. Hence, a comparison can be made between both result to define the variables that affect the mechanical properties for the single struts.

REFERENCES

3dsystems.com. (2018). CubePro 3D Printer - Technical Specifications - 3D Systems. https://www.3dsystems.com/shop/cubepro/techspecs [Accessed 25 Oct. 2018].

Doyoyo, M. and Hu, J. (2006). Multi-axial failure of metallic strut-lattice materials composed of short and slender struts. *International Journal of Solids and Structures*, 43(20), pp.6115-6139.

Gebhardt, A. (2003). Rapid prototyping. Munich: Hanser Publishers.

Halil Ibrahin Kurt and Ramazan Samur. (2013). Study on microstructure, Tensile Test and Hardness 304 Stainless Steel Jointed by TIG Welding. *International Journal of Science and Technology Volume 2 No. 2.*

Kessler, J., Bâlc, N., Gebhardt, A., & Abbas, K. (2016). Basic Research on Lattice Structures Focused on the strut shape and welding beads. *Physics Procedia*, 83, 833–838.

Rafidah Hassan (2013). Progressive Collapse of Titanium Alloy Micro-Lattice Structures Manufactured Using Selective Laser Melting.

Rashed, M., Ashraf, M., Mines, R. and Hazell, P. (2016). Metallic microlattice materials: A current state of the art on manufacturing, mechanical properties and applications. *Materials & Design*, 95, pp.518-533.

Reinhart, G., Teufelhart, S., & Riss, F. (2012). Investigation of the Geometry-dependent Anisotropic Material Behavior of Filigree Struts in ALM-produced Lattice Structures. *Physics Procedia*, 39, 471–479.

Shimadzhu (2018). Universal test – Ez Test - Specification

https://www.shimadzu.com/an/test/universal/eztest.html (Accessed 20 november 2018)

Syam, W., Jianwei, W., Zhao, B., Maskery, I., Elmadih, W. and Leach, R. (2017). Design and analysis of strut-based lattice structures for vibration isolation. *Precision Engineering*, 24, 510-523.

Tang, Y., Dong, G., Zhou, Q., & Zhao, Y. (2017). Lattice Structure Design and Optimization With Additive Manufacturing Constraints. *IEEE Transactions On Automation Science And Engineering*, 1-17.

Tsopanos, S., Mines, R.A.W., McKown, S., Shen, Y., Cantwell, W. J., Brooks, W., & Sutcliffe, C. J. (2010). The influence of processing parameters on the mechanical properties of selectively laser melted stainless steel microlatticestructures. *Journal of Manufacturing Science and Engineering*, 132: 041011-1 - 140111-12.

Van Der Klift, F., Koga, Y., Todoroki, A., Ueda, M., Hirano, Y., & Matsuzaki, R. (2015). 3D printing of continuous carbon fibre reinforced thermo-plastic (CFRTP) tensile test specimens. *Open Journal of Composite Materials*, *6*(01), 18.

APPENDICES

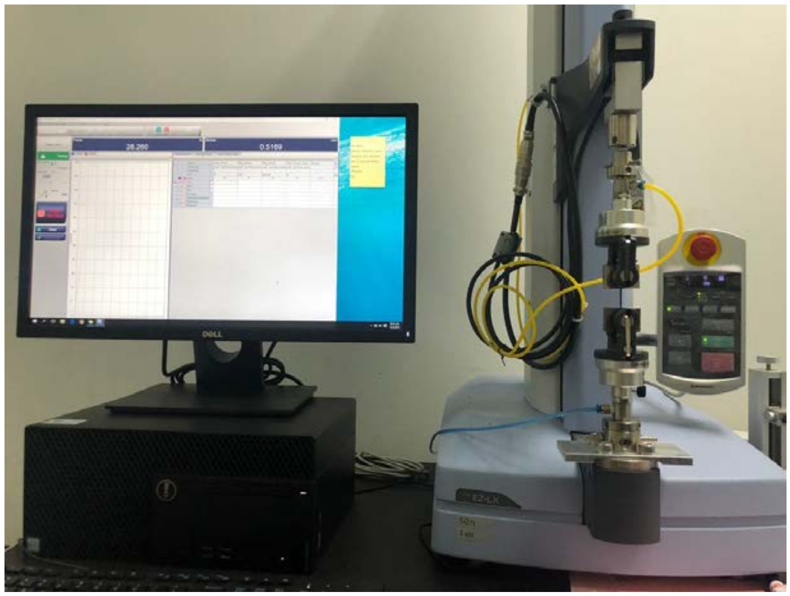

Figure A1: The setup of Shimadzhu EZ-LX tensile test by using Trapezium software.

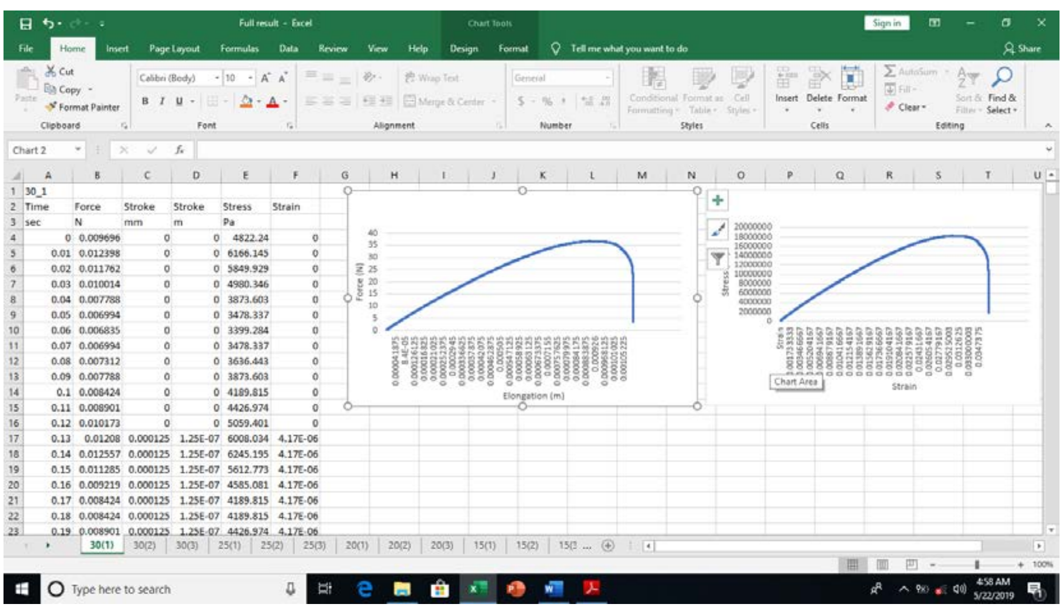

Figure A2: The raw data obtained from tensile test for 30 mm gauge length specimen one.

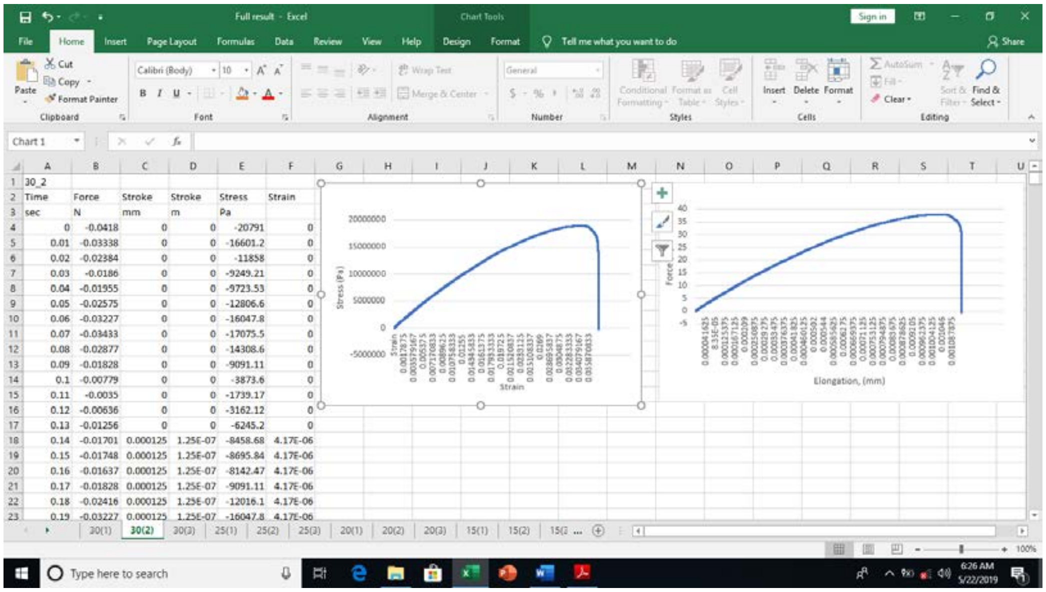

Figure A3: The raw data obtained from tensile test for 30 mm gauge length specimen two.

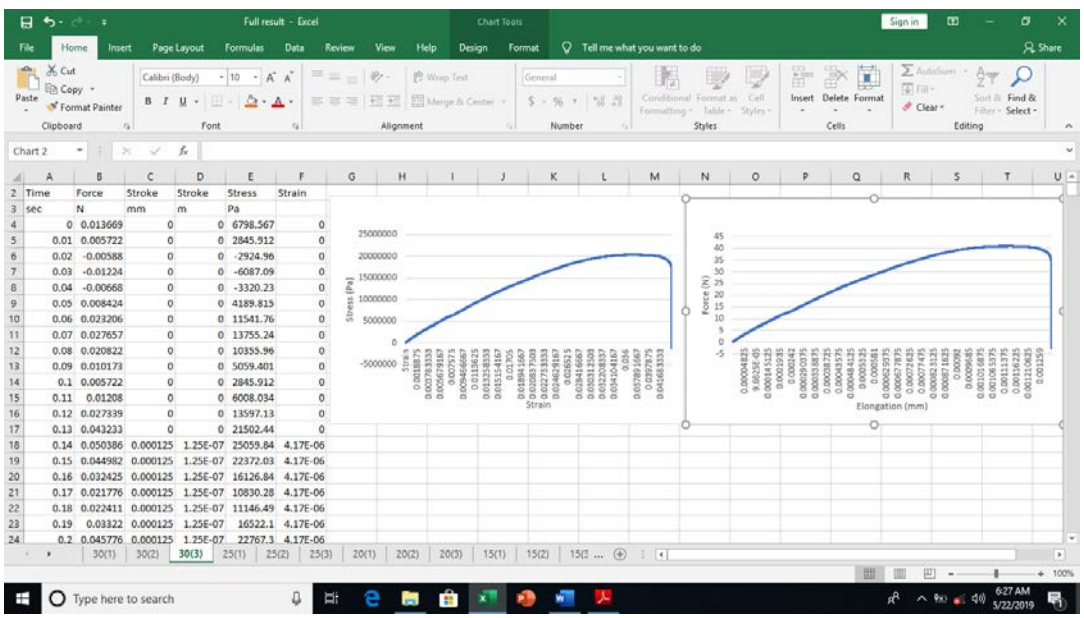

Figure A4: The raw data obtained from tensile test for 30 mm gauge length specimen three.

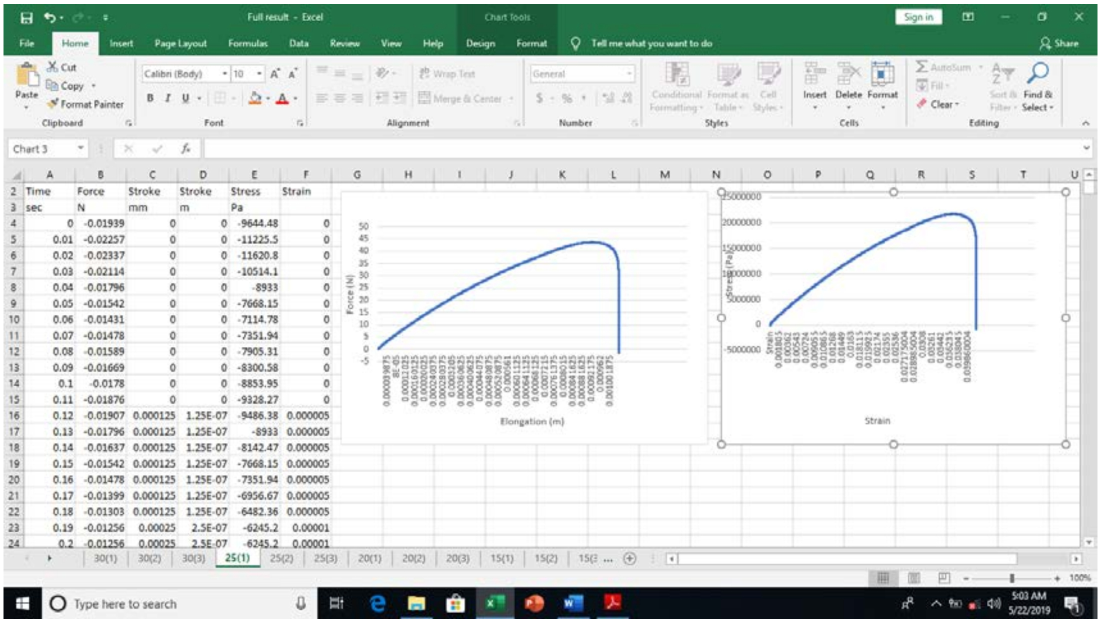

Figure A5: The raw data obtained from tensile test for 25 mm gauge length specimen one.

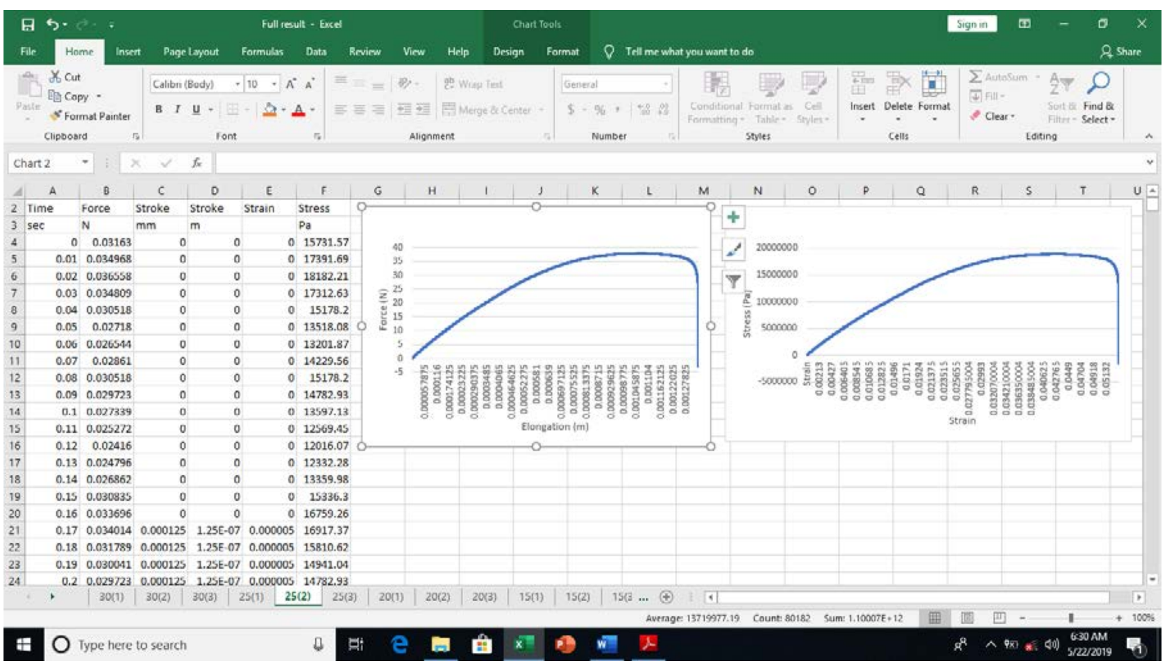

Figure A6: The raw data obtained from tensile test for 25 mm gauge length specimen two.

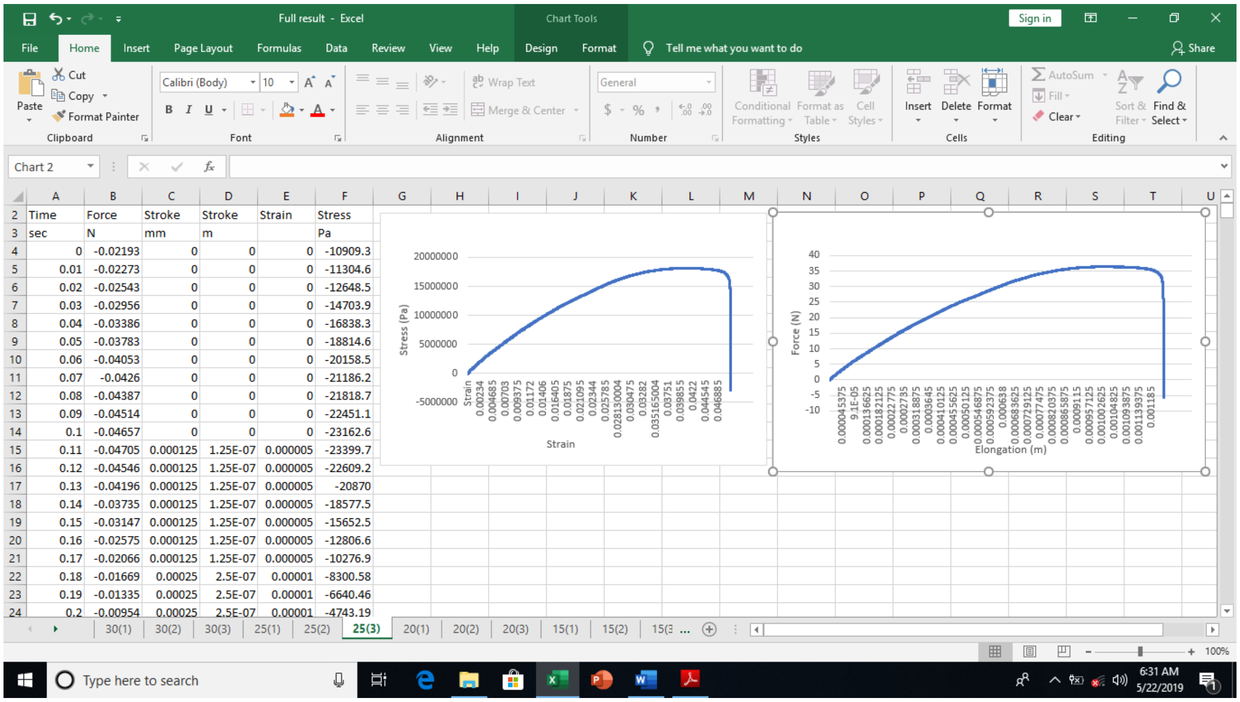

Figure A7: The raw data obtained from tensile test for 25 mm gauge length specimen three.

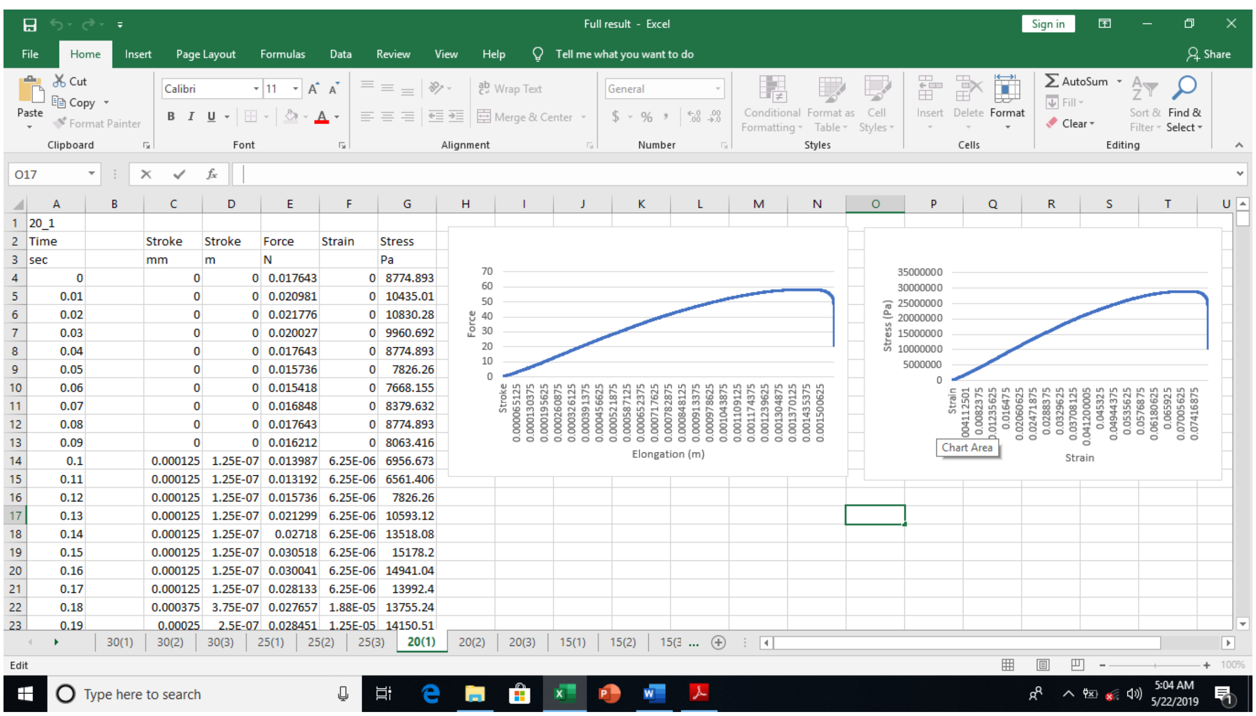

Figure A8: The raw data obtained from tensile test for 20 mm gauge length specimen one.

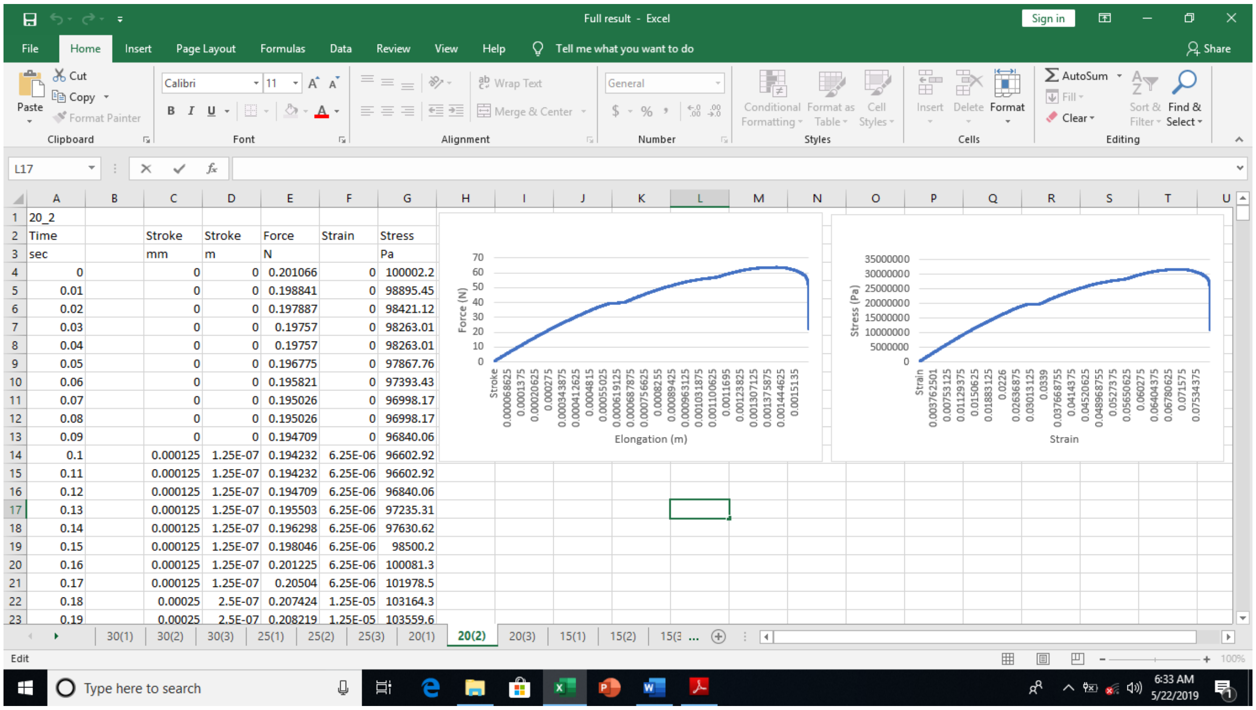

	A	B	C	D	E	F	G
1	20_2						
2	Time		Stroke	Stroke	Force	Strain	Stress
3	sec		mm	m	N		Pa
4	0		0	0	0.201066	0	100002.2
5	0.01		0	0	0.198841	0	98895.45
6	0.02		0	0	0.197887	0	98421.12
7	0.03		0	0	0.19757	0	98263.01
8	0.04		0	0	0.19757	0	98263.01
9	0.05		0	0	0.196775	0	97867.76
10	0.06		0	0	0.195821	0	97393.43
11	0.07		0	0	0.195026	0	96998.17
12	0.08		0	0	0.195026	0	96998.17
13	0.09		0	0	0.194709	0	96840.06
14	0.1		0.000125	1.25E-07	0.194232	6.25E-06	96602.92
15	0.11		0.000125	1.25E-07	0.194232	6.25E-06	96602.92
16	0.12		0.000125	1.25E-07	0.194709	6.25E-06	96840.06
17	0.13		0.000125	1.25E-07	0.195503	6.25E-06	97235.31
18	0.14		0.000125	1.25E-07	0.196298	6.25E-06	97630.62
19	0.15		0.000125	1.25E-07	0.198046	6.25E-06	98500.2
20	0.16		0.000125	1.25E-07	0.201225	6.25E-06	100081.3
21	0.17		0.000125	1.25E-07	0.20504	6.25E-06	101978.5
22	0.18		0.00025	2.5E-07	0.207424	1.25E-05	103164.3
23	0.19		0.00025	2.5E-07	0.208219	1.25E-05	103559.6

Figure A9: The raw data obtained from tensile test for 20 mm gauge length specimen two.

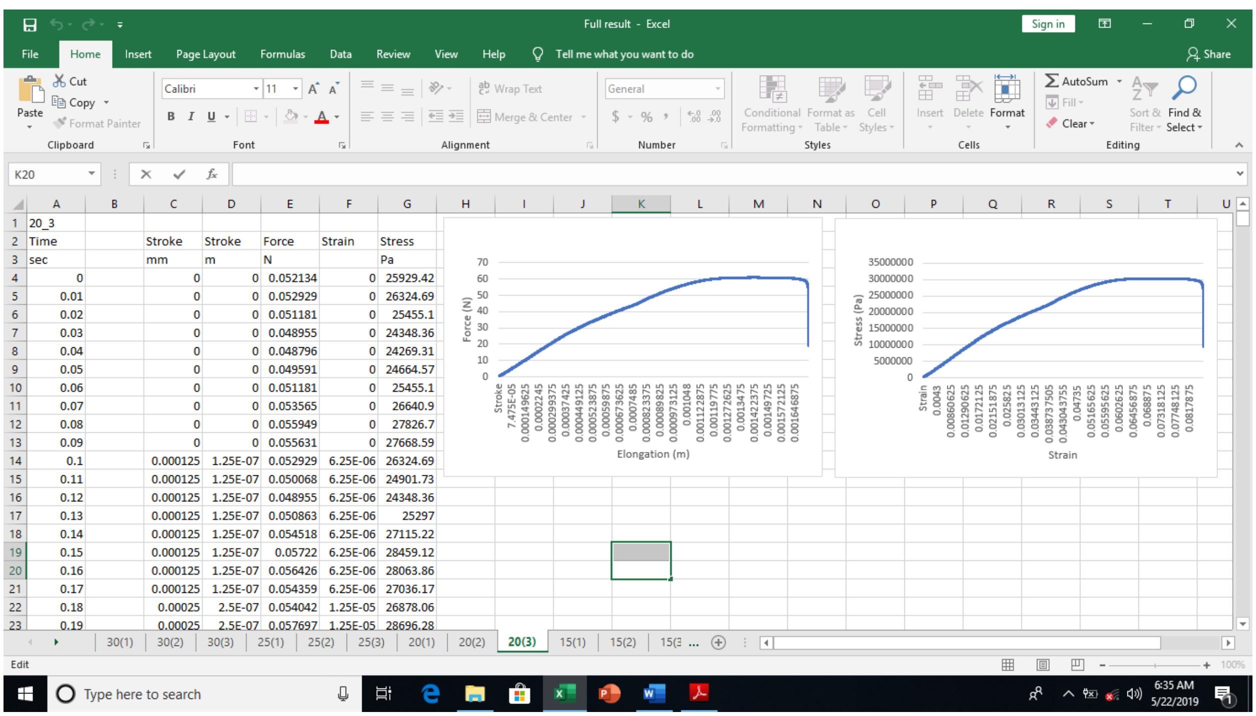

	A	B	C	D	E	F	G
1	20_3						
2	Time		Stroke	Stroke	Force	Strain	Stress
3	sec		mm	m	N		Pa
4	0		0	0	0.052134	0	25929.42
5	0.01		0	0	0.052929	0	26324.69
6	0.02		0	0	0.051181	0	25455.1
7	0.03		0	0	0.048955	0	24348.36
8	0.04		0	0	0.048796	0	24269.31
9	0.05		0	0	0.049591	0	24664.57
10	0.06		0	0	0.051181	0	25455.1
11	0.07		0	0	0.053565	0	26640.9
12	0.08		0	0	0.055949	0	27826.7
13	0.09		0	0	0.055631	0	27668.59
14	0.1		0.000125	1.25E-07	0.052929	6.25E-06	26324.69
15	0.11		0.000125	1.25E-07	0.050068	6.25E-06	24901.73
16	0.12		0.000125	1.25E-07	0.048955	6.25E-06	24348.36
17	0.13		0.000125	1.25E-07	0.050863	6.25E-06	25297
18	0.14		0.000125	1.25E-07	0.054518	6.25E-06	27115.22
19	0.15		0.000125	1.25E-07	0.05722	6.25E-06	28459.12
20	0.16		0.000125	1.25E-07	0.056426	6.25E-06	28063.86
21	0.17		0.000125	1.25E-07	0.054359	6.25E-06	27036.17
22	0.18		0.00025	2.5E-07	0.054042	1.25E-05	26878.06
23	0.19		0.00025	2.5E-07	0.057697	1.25E-05	28696.28

Figure A10: The raw data obtained from tensile test for 20 mm gauge length specimen three.

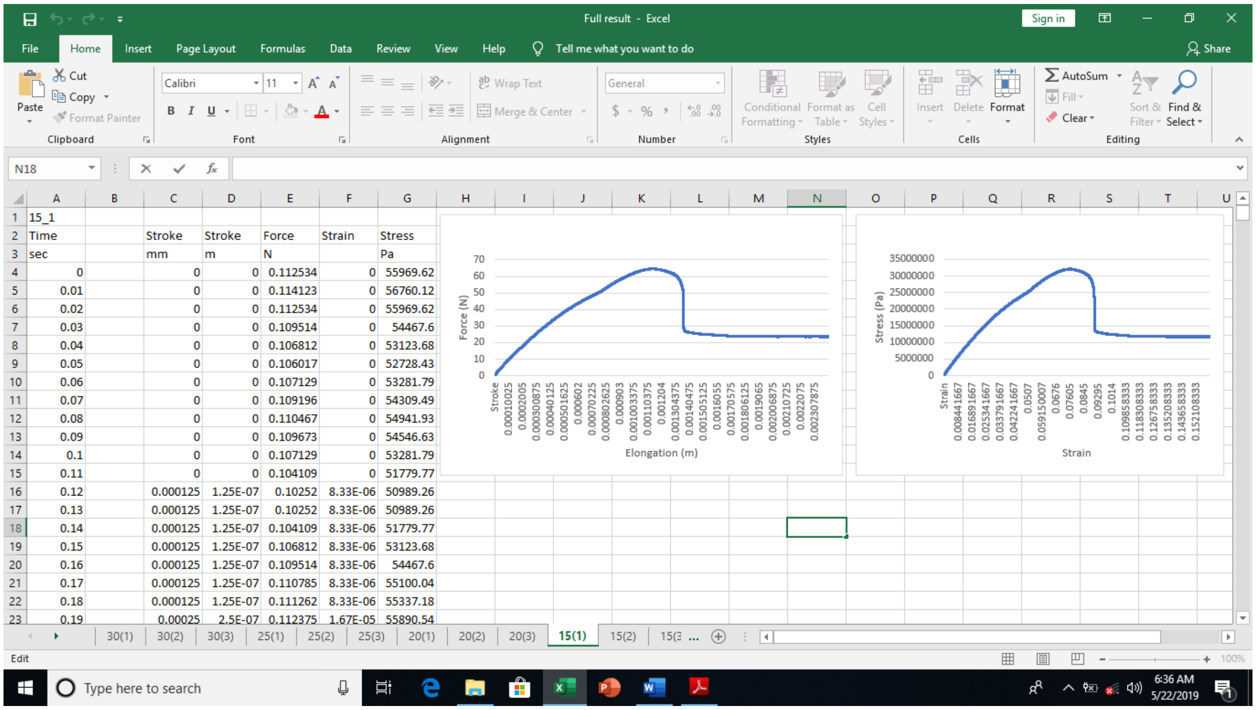

	A	B	C	D	E	F	G
1	15_1						
2	Time		Stroke	Stroke	Force	Strain	Stress
3	sec		mm	m	N		Pa
4	0		0	0	0.112534	0	55969.62
5	0.01		0	0	0.114123	0	56760.12
6	0.02		0	0	0.112534	0	55969.62
7	0.03		0	0	0.109514	0	54467.6
8	0.04		0	0	0.106812	0	53123.68
9	0.05		0	0	0.106017	0	52728.43
10	0.06		0	0	0.107129	0	53281.79
11	0.07		0	0	0.109196	0	54309.49
12	0.08		0	0	0.110467	0	54941.93
13	0.09		0	0	0.109673	0	54546.63
14	0.1		0	0	0.107129	0	53281.79
15	0.11		0	0	0.104109	0	51779.77
16	0.12		0.000125	1.25E-07	0.10252	8.33E-06	50989.26
17	0.13		0.000125	1.25E-07	0.10252	8.33E-06	50989.26
18	0.14		0.000125	1.25E-07	0.104109	8.33E-06	51779.77
19	0.15		0.000125	1.25E-07	0.106812	8.33E-06	53123.68
20	0.16		0.000125	1.25E-07	0.109514	8.33E-06	54467.6
21	0.17		0.000125	1.25E-07	0.110785	8.33E-06	55100.04
22	0.18		0.000125	1.25E-07	0.111262	8.33E-06	55337.18
23	0.19		0.00025	2.5E-07	0.112375	1.67E-05	55890.54

Figure A11: The raw data obtained from tensile test for 15 mm gauge length specimen one.

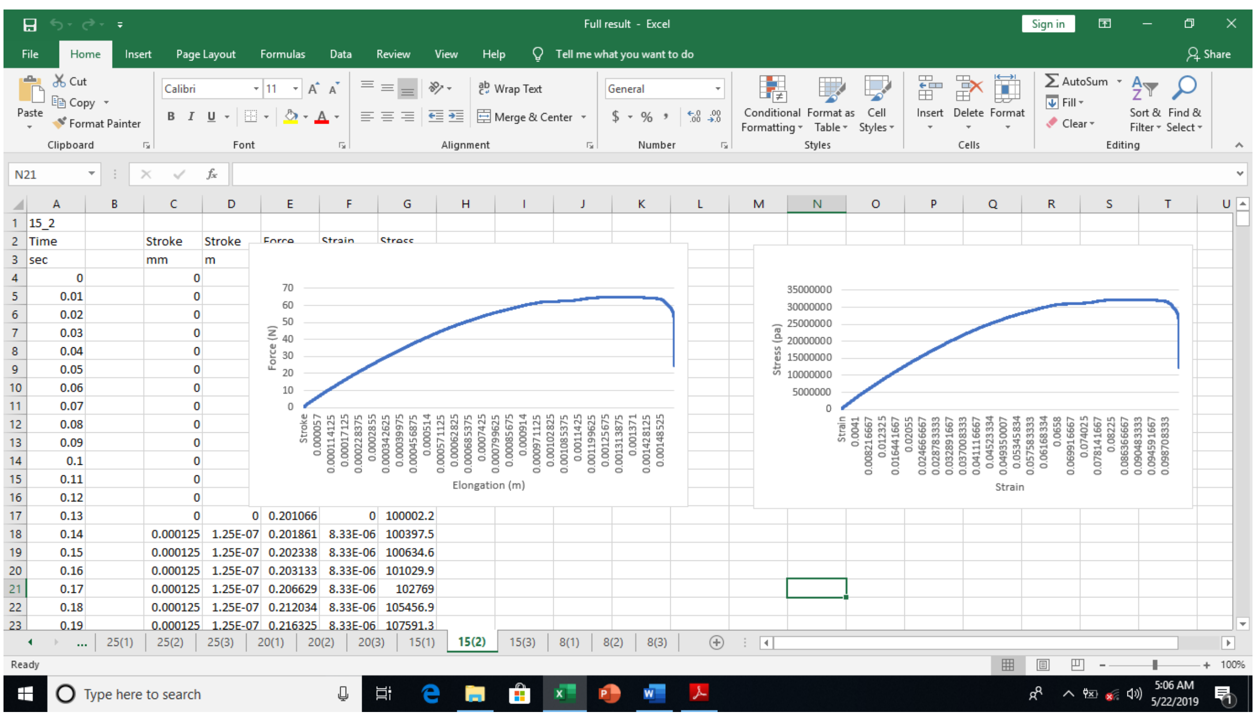

	A	B	C	D	E	F	G
1	15_2						
2	Time		Stroke	Stroke	Force	Strain	Stress
3	sec		mm	m			
4	0		0				
5	0.01		0				
6	0.02		0				
7	0.03		0				
8	0.04		0				
9	0.05		0				
10	0.06		0				
11	0.07		0				
12	0.08		0				
13	0.09		0				
14	0.1		0				
15	0.11		0				
16	0.12		0				
17	0.13		0	0	0.201066	0	100002.2
18	0.14		0.000125	1.25E-07	0.201861	8.33E-06	100397.5
19	0.15		0.000125	1.25E-07	0.202338	8.33E-06	100634.6
20	0.16		0.000125	1.25E-07	0.203133	8.33E-06	101029.9
21	0.17		0.000125	1.25E-07	0.206629	8.33E-06	102769
22	0.18		0.000125	1.25E-07	0.212034	8.33E-06	105456.9
23	0.19		0.000125	1.25E-07	0.216325	8.33E-06	107591.3

Figure A12: The raw data obtained from tensile test for 15 mm gauge length specimen two.

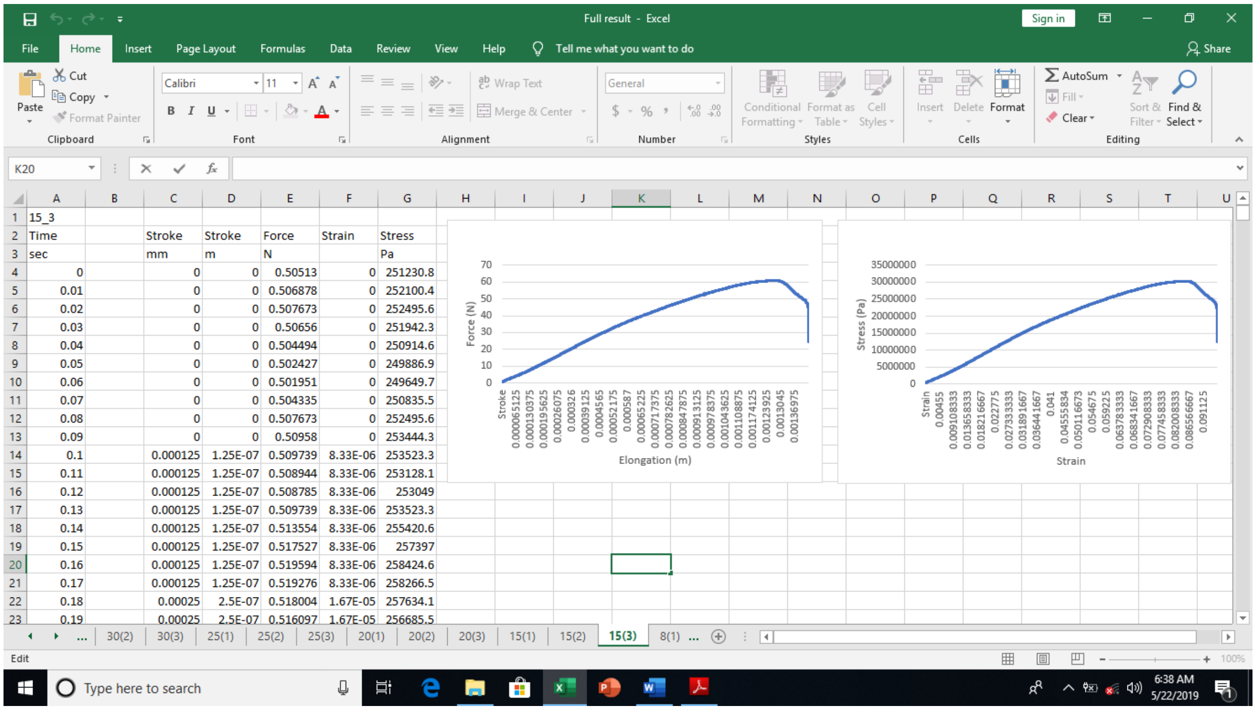

	A	B	C	D	E	F	G
1	15_3						
2	Time		Stroke	Stroke	Force	Strain	Stress
3	sec		mm	m	N		Pa
4	0		0	0	0.50513	0	251230.8
5	0.01		0	0	0.506878	0	252100.4
6	0.02		0	0	0.507673	0	252495.6
7	0.03		0	0	0.50656	0	251942.3
8	0.04		0	0	0.504494	0	250914.6
9	0.05		0	0	0.502427	0	249886.9
10	0.06		0	0	0.501951	0	249649.7
11	0.07		0	0	0.504335	0	250835.5
12	0.08		0	0	0.507673	0	252495.6
13	0.09		0	0	0.50958	0	253444.3
14	0.1		0.000125	1.25E-07	0.509739	8.33E-06	253523.3
15	0.11		0.000125	1.25E-07	0.508944	8.33E-06	253128.1
16	0.12		0.000125	1.25E-07	0.508785	8.33E-06	253049
17	0.13		0.000125	1.25E-07	0.509739	8.33E-06	253523.3
18	0.14		0.000125	1.25E-07	0.513554	8.33E-06	255420.6
19	0.15		0.000125	1.25E-07	0.517527	8.33E-06	257397
20	0.16		0.000125	1.25E-07	0.519594	8.33E-06	258424.6
21	0.17		0.000125	1.25E-07	0.519276	8.33E-06	258266.5
22	0.18		0.00025	2.5E-07	0.518004	1.67E-05	257634.1
23	0.19		0.00025	2.5E-07	0.516097	1.67E-05	256685.5

Figure A13: The raw data obtained from tensile test for 15 mm gauge length specimen three.

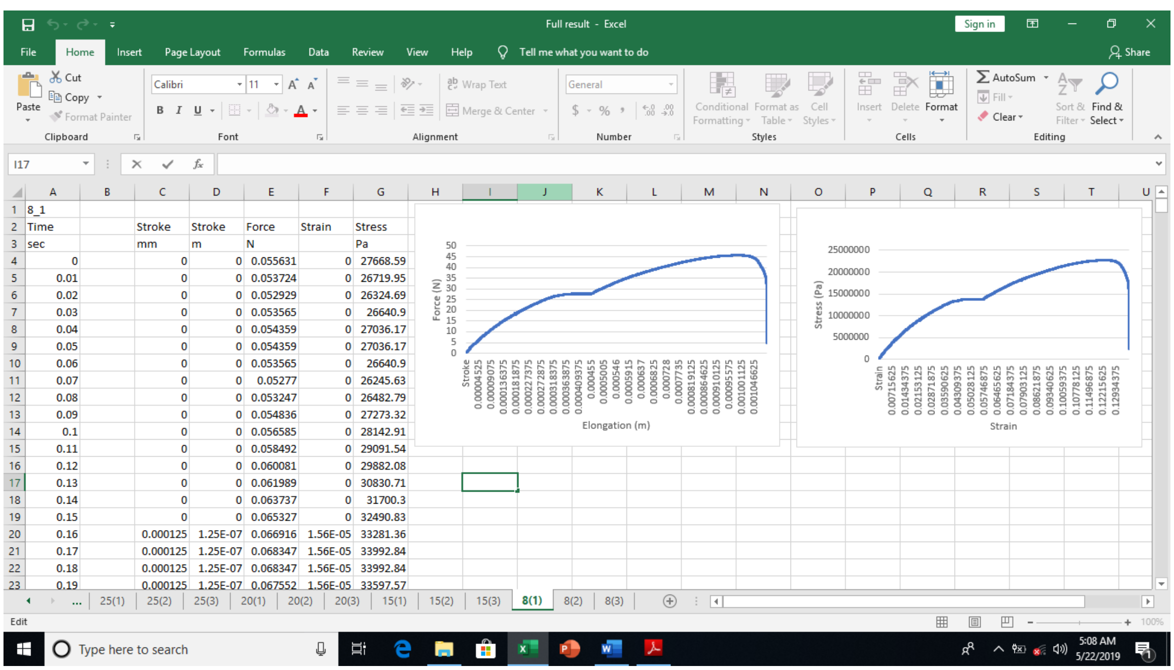

	A	B	C	D	E	F	G
1	8_1						
2	Time		Stroke	Stroke	Force	Strain	Stress
3	sec		mm	m	N		Pa
4	0		0	0	0.055631	0	27668.59
5	0.01		0	0	0.053724	0	26719.95
6	0.02		0	0	0.052929	0	26324.69
7	0.03		0	0	0.053565	0	26640.9
8	0.04		0	0	0.054359	0	27036.17
9	0.05		0	0	0.054359	0	27036.17
10	0.06		0	0	0.053565	0	26640.9
11	0.07		0	0	0.05277	0	26245.63
12	0.08		0	0	0.053247	0	26482.79
13	0.09		0	0	0.054836	0	27273.32
14	0.1		0	0	0.056585	0	28142.91
15	0.11		0	0	0.058492	0	29091.54
16	0.12		0	0	0.060081	0	29882.08
17	0.13		0	0	0.061989	0	30830.71
18	0.14		0	0	0.063737	0	31700.3
19	0.15		0	0	0.065327	0	32490.83
20	0.16		0.000125	1.25E-07	0.066916	1.56E-05	33281.36
21	0.17		0.000125	1.25E-07	0.068347	1.56E-05	33992.84
22	0.18		0.000125	1.25E-07	0.068347	1.56E-05	33992.84
23	0.19		0.000125	1.25E-07	0.067552	1.56E-05	33597.57

Figure A14: The raw data obtained from tensile test for 8 mm gauge length specimen one.

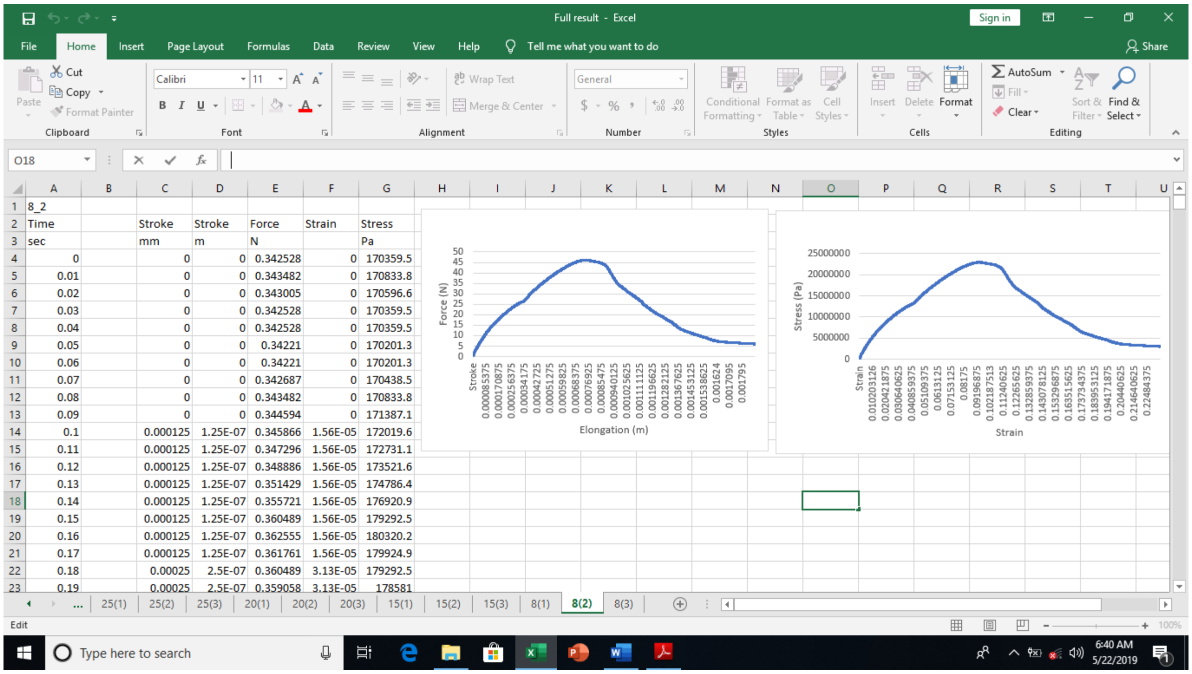

	Time		Stroke	Stroke	Force	Strain	Stress
1	8_2						
2	Time		Stroke	Stroke	Force	Strain	Stress
3	sec		mm	m	N		Pa
4	0		0	0	0.342528	0	170359.5
5	0.01		0	0	0.343482	0	170833.8
6	0.02		0	0	0.343005	0	170596.6
7	0.03		0	0	0.342528	0	170359.5
8	0.04		0	0	0.342528	0	170359.5
9	0.05		0	0	0.34221	0	170201.3
10	0.06		0	0	0.34221	0	170201.3
11	0.07		0	0	0.342687	0	170438.5
12	0.08		0	0	0.343482	0	170833.8
13	0.09		0	0	0.344594	0	171387.1
14	0.1		0.000125	1.25E-07	0.345866	1.56E-05	172019.6
15	0.11		0.000125	1.25E-07	0.347296	1.56E-05	172731.1
16	0.12		0.000125	1.25E-07	0.348886	1.56E-05	173521.6
17	0.13		0.000125	1.25E-07	0.351429	1.56E-05	174786.4
18	0.14		0.000125	1.25E-07	0.355721	1.56E-05	176920.9
19	0.15		0.000125	1.25E-07	0.360489	1.56E-05	179292.5
20	0.16		0.000125	1.25E-07	0.362555	1.56E-05	180320.2
21	0.17		0.000125	1.25E-07	0.361761	1.56E-05	179924.9
22	0.18		0.00025	2.5E-07	0.360489	3.13E-05	179292.5
23	0.19		0.00025	2.5E-07	0.359058	3.13E-05	178581

Figure A15: The raw data obtained from tensile test for 8 mm gauge length specimen two.

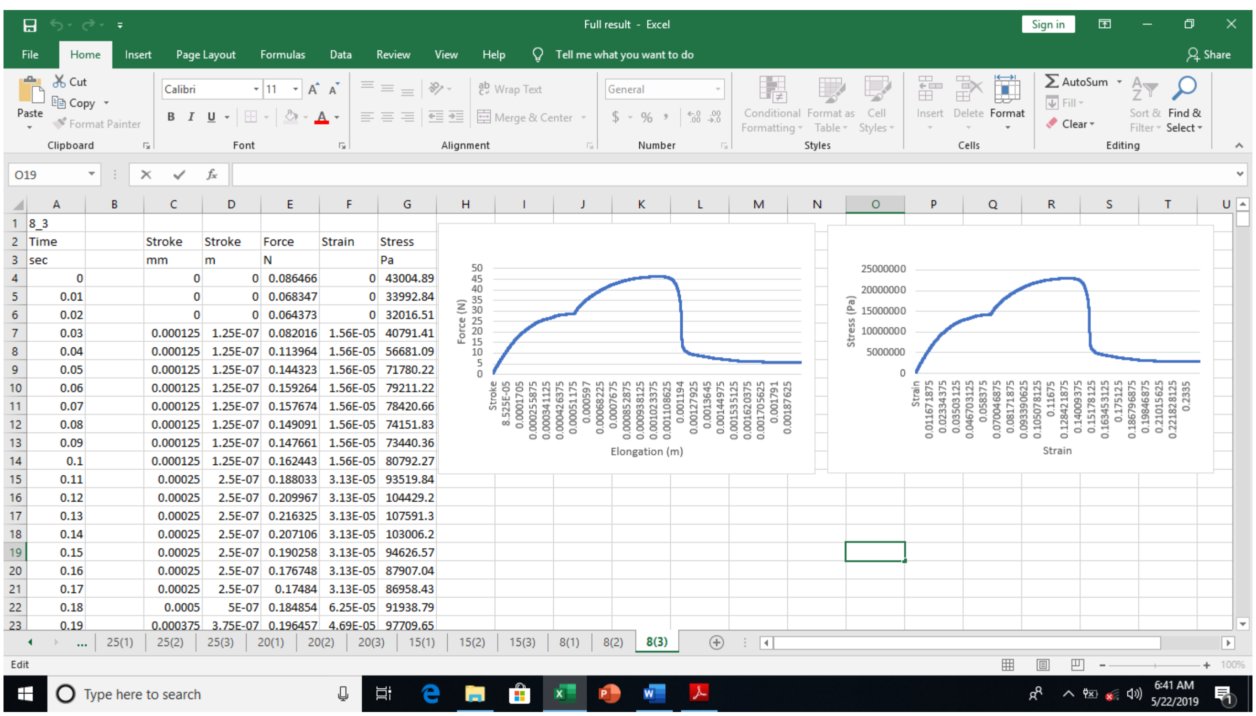

	Time		Stroke	Stroke	Force	Strain	Stress
1	8_3						
2	Time		Stroke	Stroke	Force	Strain	Stress
3	sec		mm	m	N		Pa
4	0		0	0	0.086466	0	43004.89
5	0.01		0	0	0.068347	0	33992.84
6	0.02		0	0	0.064373	0	32016.51
7	0.03		0.000125	1.25E-07	0.082016	1.56E-05	40791.41
8	0.04		0.000125	1.25E-07	0.113964	1.56E-05	56681.09
9	0.05		0.000125	1.25E-07	0.144323	1.56E-05	71780.22
10	0.06		0.000125	1.25E-07	0.159264	1.56E-05	79211.22
11	0.07		0.000125	1.25E-07	0.157674	1.56E-05	78420.66
12	0.08		0.000125	1.25E-07	0.149091	1.56E-05	74151.83
13	0.09		0.000125	1.25E-07	0.147661	1.56E-05	73440.36
14	0.1		0.000125	1.25E-07	0.162443	1.56E-05	80792.27
15	0.11		0.00025	2.5E-07	0.188033	3.13E-05	93519.84
16	0.12		0.00025	2.5E-07	0.209967	3.13E-05	104429.2
17	0.13		0.00025	2.5E-07	0.216325	3.13E-05	107591.3
18	0.14		0.00025	2.5E-07	0.207106	3.13E-05	103006.2
19	0.15		0.00025	2.5E-07	0.190258	3.13E-05	94626.57
20	0.16		0.00025	2.5E-07	0.176748	3.13E-05	87907.04
21	0.17		0.00025	2.5E-07	0.17484	3.13E-05	86958.43
22	0.18		0.0005	5E-07	0.184854	6.25E-05	91938.79
23	0.19		0.000375	3.75E-07	0.196457	4.69E-05	97709.65

Figure A16: The raw data obtained from tensile test for 8 mm gauge length specimen three.